

# Electron Transfer Partners of Cytochrome P450

# 2

Lucy Waskell and Jung-Ja P. Kim

## Abbreviations

POR	NADPH-cytochrome P450 oxidoreductase
<i>POR</i>	POR gene
P450	Cytochrome P450
cyt <i>c</i>	Cytochrome <i>c</i>
cyt <i>b</i> <sub>5</sub>	Cytochrome <i>b</i> <sub>5</sub>
NOS	Nitric oxide synthase
FNR	Ferredoxin-NADP <sup>+</sup> reductase
Fld	Flavodoxin
FMN domain	FMN-containing flavodoxin-like domain
FAD domain	FAD-containing FNR-like domain plus the connecting domain
P450BM3	<i>Bacillus megaterium</i> flavocytochrome P450BM3
MS	Methionine synthase
MSR	Methionine synthase reductase
ER	Endoplasmic reticulum
HO	Heme oxygenase

## 2.1 Introduction

Cytochrome P450 (P450) electron transport is mediated by a multicomponent monooxygenase system, in which reducing equivalents from NADPH (Nicotinamide Adenine Dinucleotide Phosphate) are transferred to molecular oxygen via one of many cytochrome P450 isozymes [1, 2]. Depending on the cellular location and their redox partners, P450s are generally divided into two major classes, class I and class II. Class I includes mitochondrial and bacterial P450s that use two separate redox partners consisting of an iron-sulfur protein (ferredoxin/adrenodoxin) and a flavin-containing reductase (ferredoxin/adrenodoxin reductase). The class II P450s are microsomal monooxygenases that receive electrons from NADPH-cytochrome P450 oxidoreductase (POR), the founding member of the diflavin reductase family. Both the reductase and the monooxygenases are integral membrane proteins. In addition, there are many minor classes of P450s reviewed in Hannemann, et al.[3], including P450 proteins that are fused to their own diflavin reductase partner in one polypeptide chain, e.g., P450BM3 from *Bacillus megaterium* (see Fig. 2.1). Most mammalian P450s are located in the endoplasmic reticulum (ER). In humans, 50 of 57 P450s are microsomal and the remaining seven are located in mitochondria. The microsomal P450s use a single POR for electron delivery from NADPH. In addition, some microsomal P450s also use cytochrome *b*<sub>5</sub> (cyt *b*<sub>5</sub>).

---

L. Waskell (✉)  
University of Michigan Medical School and VA Medical  
Center, Ann Arbor, MI, USA  
e-mail: waskell@med.umich.edu

J.-J. P. Kim  
Department of Biochemistry, Medical College  
of Wisconsin, Milwaukee, WI, USA  
e-mail: jjkim@mcw.edu

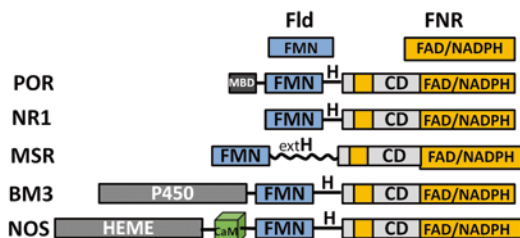


**Fig. 2.1** Domain organization of NADPH-cytochrome P450 oxidoreductase (*POR*) and other members of the diflavin oxidoreductase family. *Fld* flavodoxin, *FNR* ferredoxin-NADP<sup>+</sup> oxidoreductase, *MBD* transmembrane domain, *H* hinge, *CD* connecting domain, *NR1* novel reductase 1, *MSR* methionine synthase reductase, which contains an ~80 residue extended hinge region (*extH*) between the FMN domain and CD, *BM3* *Bacillus megaterium* flavocytochrome P450, *NOS* nitric oxide synthase, which has a calmodulin-binding region (CaM). Note that the CD consists of two noncontiguous parts of the linear sequence interspersed with the FNR-like domain

*POR* is a membrane-bound ~78-kDa protein. *POR* is the prototypic member of the diflavin oxidoreductase family of enzymes that contain one molecule each of flavin adenine dinucleotide (FAD) and flavin mononucleotide (FMN) in a single polypeptide. These enzymes perform a step-down function, i.e., transferring electrons from the two-electron donor NADPH to one-electron acceptors (e.g., heme), with the FAD functioning as a dehydrogenase flavin and FMN as an electron carrier. In other words, NADPH transfers a hydride ion to the FAD, which transfers these two electrons one at a time to the FMN. It is the FMN hydroquinone that is the ultimate electron donor, again one by one, to P450 and other electron transfer partners. Other prominent members of this family are the reductase domains of the nitric oxide synthase (*NOS*) isozymes (reviewed in [4–7] and flavocytochrome P450BM3 (*P450BM3*) from *Bacillus megaterium* [8], and the flavoprotein subunits of bacterial sulfite reductase[9], all of which transfer electrons to heme, as well as methionine synthase reductase (*MSR*), which reduces Cob(II)alamin of methionine synthase [10–12], human cancer-related novel reductase 1 (*NR1*) [13], pyruvate: NADP<sup>+</sup> oxidoreductase from *Euglena gracilis* [14, 15], and reductase Tah18 protein from yeast [16]. The domain structures of these proteins are all similar to that of *POR*, containing the flavodoxin (*Fld*)-

like and ferredoxin-NADP<sup>+</sup> reductase (*FNR*)-like folds, having similar functions and mechanisms of action (Figs. 2.1 and 2.2).

*POR* functions to transfer electrons from NADPH to a number of microsomal electron acceptors, including not only P450s but also heme oxygenase (HO) [17], *cyt b<sub>5</sub>* [18], squalene monooxygenase [19], and possibly indole dioxygenase [20]. In addition, a number of nonphysiological electron acceptors, including cytochrome *c* (*cyt c*), ferricyanide, menadione, and dichloroindophenol, have been used for biochemical characterization of the enzyme. On the other hand, other members of the diflavin oxidoreductase family, including *MSR*, *NOS*, and *P450BM3*, transfer electrons to a single physiological acceptor. For *NOS* and *P450BM3*, both the donor and acceptor are located on the same polypeptide (Fig. 2.1). However, both *NOS* and *P450BM3* are dimeric molecules and the reductase domain of monomer 1 reduces the heme domain of monomer 2 and vice versa. The electron acceptors for *POR*, including the multiplicity of P450s, as well as other protein acceptors listed above, are located in the ER, and the levels of *POR* are substantially lower than those of its acceptors, with the ratio of *POR* to P450 in liver ER estimated at 1:5~20 [21–23]. Although the large and diverse family of P450s exhibits a common fold in the vicinity of the heme ligand, each P450 also possesses unique structural features, substrate specificity, and rate-limiting catalytic steps [24, 25]. Thus, electron transfer to all these proteins must proceed in a finely controlled fashion. The question arises as to how *POR* recognizes and mediates electron transfer to this multiplicity of electron acceptors.

This chapter discusses the mechanism of interaction between P450s and their redox partners, primarily the diflavin oxidoreductase, *POR*, and *cyt b<sub>5</sub>*. The domain organization and the high degree of conformational changes in *POR* necessary for the precise orchestration of electron transfer to its >50 different electron acceptors will be highlighted. The complex and controversial role of *cyt b<sub>5</sub>* as a redox partner for P450 will also be discussed. Details of the reaction of a Class I P450 with an iron sulfur protein are provided in the chapter by Poulos and Johnson.

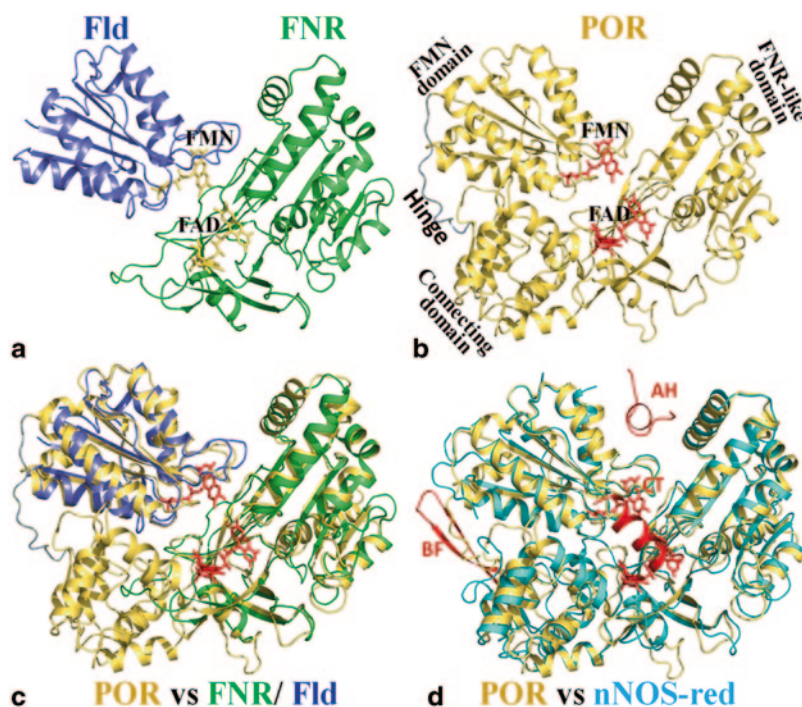


**Fig. 2.2** Evolutionary origins of the structures of NADPH-cytochrome P450 oxidoreductase (*POR*) and the neuronal NOS (*nNOS*) reductase domain (*cyan*), shown by overlays of the ribbon structures of *Desulfovibrio vulgaris* flavodoxin (*Fld*) and spinach ferredoxin-NADP-oxidoreductase (*FNR*). **a** Structures of *Fld* and *FNR*. **b** *POR* with flavin mononucleotide (*FMN*) and flavin adenine dinucleotide (*FAD*) highlighted with red sticks. The

*FMN* domain, *FNR*-like domain, connecting domain, and the flexible hinge are marked. **c** Overlay of the structures of *Fld*, *FNR*, and *POR*. The connecting domain and hinge are unique to *POR*. **d** Overlay of *POR* and *nNOS*-red. The *nNOS* reductase domain [40] contains various regulatory elements, including the autoregulatory insert (*AR*),  $\beta$ -finger (*BF*), and the C-terminal extension (*CT*). They are shown in red

## 2.2 NADPH-Cytochrome P450 Oxidoreductase

### 2.2.1 Properties of POR Flavins

The ability of flavins to engage in both 1-electron and 2-electron redox chemistry is key to their functions in electron transfer. In *POR*, they are an essential intermediate between NADPH, a two-electron donor, and the heme of P450, a one-electron acceptor. Furthermore, utilization of two flavins, located in separate domains, provides a mechanism for control of the kinetics of electron transfer by regulating the distance between, and the relative orientation of, the two flavins. The flavin cofactors can exist as the oxidized (ox), one-electron reduced semiquinone (sq), and two-electron, fully reduced (red) forms (Fig. 2.3).

Both the semiquinone and the fully reduced forms can exist free in solution as either neutral or anionic forms with  $pK_a$  values of 8.5 and 6.5, respectively. Both semiquinones of *POR* are found as the blue, neutral form in the pH range 6.5–8.5. In this review, the fully reduced forms are referred to as  $FMNH_2$  and  $FADH_2$ . However, the protonation states of the fully reduced forms in *POR* are unknown. Those of the homologous proteins, *FNR* and flavodoxin, are anionic and it should be kept in mind that the fully reduced flavins in *POR* may also be in the anionic forms,  $FADH^-$  and  $FMNH^-$ .

The oxidation and protonation states of the flavins can be distinguished by their distinct visible absorption spectra, which have been invaluable in characterizing the oxidation states of flavoproteins during catalysis [7, 26, 27]. Oxi-

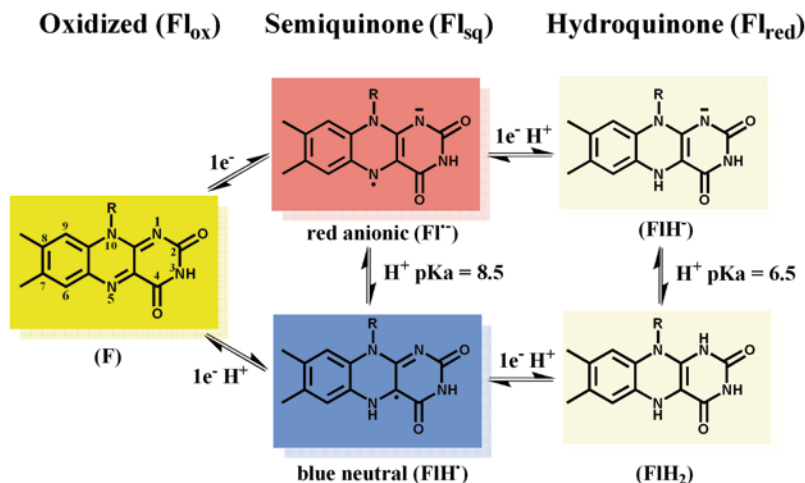


**Fig. 2.3** Various redox states of the isoalloxazine ring of flavin mononucleotide (FMN) and flavin adenine dinucleotide (FAD). The background color for each redox state represents its visible spectrum

dized flavins have broad absorption maxima at approximately 450 and 380 nm. The neutral blue semiquinones are characterized by a broad absorbance between 500 and 700 nm, with maxima in the region between 585 and 600 nm. In POR, the FMN, but not the FAD, semiquinone has a shoulder at 630 nm, which enables discrimination of the FADH<sup>•</sup> and FMNH<sup>•</sup> semiquinones and analysis of one-electron transfer reactions between FAD and FMN [27]. The FMNH<sup>•</sup> semiquinone is air stable, while the FADH<sup>•</sup> semiquinone is unstable and rapidly oxidizes in air. The stability of the neutral FMNH<sup>•</sup> semiquinone is likely due to a hydrogen bond between N5 of the FMN and the main chain carbonyl group of a highly conserved glycine residue in a nearby loop (Gly141 in rat POR).

The reduction potentials of the POR flavins have been determined for the rabbit [28], rat [29], and human [30, 31] enzymes. For FMN,  $\Delta E_{ox/sq} = -110 \sim -66$  mV and  $\Delta E_{sq/red} = -246 \sim -290$  mV; for FAD,  $\Delta E_{ox/sq} = -290 \sim -328$  mV and  $\Delta E_{sq/red} = -372 \sim -382$  mV. Although there are some variations in reduction potentials between species, the FAD semiquinone/reduced couple always exhibits a low reduction potential ( $\sim -380$  mV), at or near that of NADPH ( $-320$  mV). Thus, FAD is the low-potential flavin and electron transfer proceeds from NADPH to FAD to FMN to P450

[32]. It should be noted that these reduction potentials have been determined for the solubilized protein in aqueous solution and, that membrane lipids and their compositions may influence the flavin reduction potentials [29].

## 2.2.2 Redox Cycling of POR Flavins

Figure 2.4 illustrates the overall reaction mechanism by which two-electrons from NADPH are transferred to the one-electron acceptor, ferric P450. Two electrons from NADPH must enter the enzyme as a hydride ion to the FAD, followed by intramolecular electron transfer to FMN. The FMN semiquinone is extremely stable, indicating that it is the hydroquinone FMN that transfers electrons to electron acceptors and that the fully oxidized enzyme form does not accumulate. The POR flavins cycle in a 1-3-2-1 electron cycle (upper half circle in Fig. 2.4a). The air-stable form, FMN<sup>•</sup>/FAD can be formed from the fully oxidized form during the priming reaction (Fig. 2.4b). At high concentrations of NADPH, the intermediate FMNH<sub>2</sub>/FAD is reduced to a four-electron reduced form [33, 34]. Since the air-stable semiquinone form is found predominantly in liver microsomes [26], the 1-3-2-1 cycle is likely the major mechanism in vivo. Although the low reduction potential of FAD, near

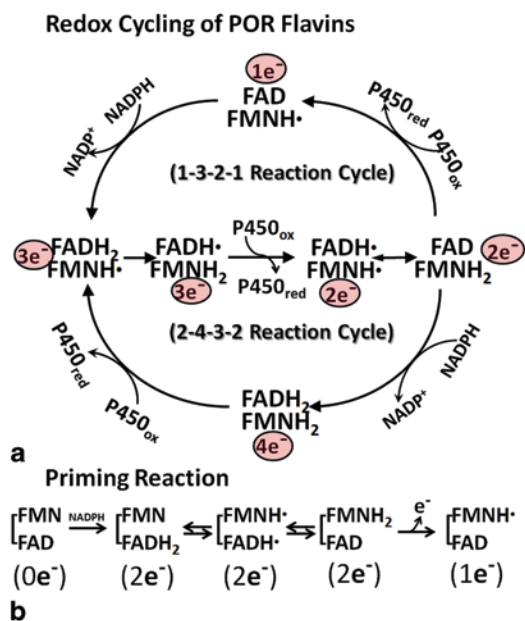


**Fig. 2.4** **a** Catalytic cycling of NADPH-cytochrome P450 oxidoreductase (*POR*) flavins. Redox cycling and electron transfer via 1-3-2-1 (*upper half circle*) and 2-4-3-2 (*lower half circle*) electron reaction cycles are shown. The *middle line* is common to both cycles. The air-stable 1e<sup>-</sup> reduced form (*FAD/FMNH•*) is obtained through the priming reaction. **b** Scheme for the priming reaction, generating the air-stable 1e<sup>-</sup> reduced form (*FAD/FMNH•*) by reduction of fully oxidized enzyme

or below that of NADPH (−320 mV), suggests that formation of the fully reduced (four-electron reduced) form of the enzyme is thermodynamically unfavorable, the 2-4-3-2 cycle is also possible depending on the NADPH/NADP<sup>+</sup> ratio [27].

### 2.2.3 Domain Structure and Function

As predicted, based on DNA sequence homology [35], *POR* likely arose from the fusion of two ancestral genes related to the flavodoxin (*Fld*) and ferredoxin NADP<sup>+</sup> reductase (*FNR*) proteins. This hypothesis has subsequently been confirmed both by site-directed mutagenesis studies and X-ray crystallography [36], confirming the structural and catalytic functions of conserved residues. The domain organization of *POR* is apparent from the crystal structure of *POR*, exhibiting domains structurally related to flavodoxin

and *FNR* (Fig. 2.2). Conservation of cofactor binding and catalytic residues is also observed. Furthermore, the fact that boundaries of the domains correspond to exon junctions in the gene encoding the enzyme is additional evidence that *POR* has arisen from a gene fusion event. The three-dimensional protein structures of spinach *FNR*, *Fld* from *Desulfovibrio vulgaris*, and rat *POR* also strongly support a common ancestor based on the very high structural similarity between the individual domains despite their very different origin [36, 37] (Fig. 2.2). The ability to express the different domains of *POR* as individual, functionally active proteins, and to successfully reconstitute these domains *in vitro* to form a functional protein complex of NADPH-cytochrome P450 oxidoreductase activity is additional evidence that *POR* has evolved as a result of gene fusion event [38, 39].

*POR* is anchored in the microsomal membrane by a ~56-amino acid N-terminal membrane binding domain (*MBD*), with the catalytic functions of *POR* residing in the soluble portion, residues 66–678 (residue numbering is based on rat *POR*, unless otherwise noted). As shown in Fig. 2.2, the structure of the soluble portion of *POR* is composed of an FMN-binding domain, which is structurally similar to *Fld*, and an FAD-binding domain. The FAD domain consists of an *FNR*-like domain with binding sites for FAD and NADPH and a connecting domain (*CD*), which is unique to *POR* and to all members of the diflavin reductase family, including nitric oxide synthases [40]. The *CD* is composed mainly of  $\alpha$  helices that connect (join) the FMN and *FNR*-like domains. The FMN and FAD domains are linked by a flexible hinge/linker (residues 232–243), consisting mostly of hydrophilic residues.

The presence of a connecting domain and hinge is unique to all members of the diflavin oxidoreductases (Fig. 2.1). Although the amino acid sequences of the connecting domains (*CDs*) exhibit low (<30%) sequence homology, there is significant structural similarity among connecting domains of different members of the diflavin family (see comparison of *POR* and *nNOS* in Fig. 2.2). Both the length and sequence of the hinge are unique for each member of this family.

The hinge plays a crucial role in POR's interaction with its electron transfer partners. It is believed that the hinge and connecting domain are largely responsible for the domain movements that control cofactor binding, interflavin electron transfer, and recognition and electron transfer to the partners (see below).

### 2.2.3.1 Membrane Binding Domain

POR is anchored to the lipid bilayer of the ER and nuclear membrane by an approximately 60 amino acid MBD. The MBD contains a 23-amino acid stretch of hydrophobic amino acids that presumably spans the lipid bilayer, followed by a stop-transfer sequence, <sup>45</sup>RKKKEE<sup>50</sup>, and a flexible segment susceptible to proteolytic cleavage [41, 42]. Cleavage by trypsin at the Lys56-Ile57 bond releases the POR from the microsomal membrane. The trypsin-cleaved protein is no longer able to transfer electrons to P450, but retains activity towards other electron acceptors such as *cyt c*. Similarly, *cyt b<sub>5</sub>* is attached to the membrane via a C-terminal MBD that is necessary for electron transfer to P450. Both passive and active roles in P450-mediated catalysis have been proposed for the MBD. Since fusion proteins, such as P450BM3 and the NOS isozymes, do not require the MBD for catalytic activity, the MBD likely serves to localize and possibly restrict movement of POR in the membrane rather than to provide a specific binding site [43–45]. In this case, the precise sequence of the membrane domain would be less important than its ability to insert into the membrane. Substitution of the POR MBD with that of *cyt b<sub>5</sub>*, which has only about 20% sequence identity, but a similar hydrophobicity profile [46], produced a chimeric POR that was able to support CYP17A-mediated P450 activity, but not CYP3A4-mediated testosterone 6 $\beta$ -hydroxylation. Taken together with the observation that the MBD of yeast POR is not required for electron transfer to P450 51 [47], it appears that the MBD may contribute to P450 recognition and binding, but is likely that only one of many POR-P450 interactions may vary depending on the specific P450.

Recently, an interesting function for the MBD has been proposed by Das and Sligar [29], showing that the flavin redox potentials are influenced by the composition of the lipid bilayer. The significance of these altered redox potentials relative to catalysis has not been demonstrated. However, lipid composition, including charge, has been reported to influence rates of P450 metabolism in reconstituted systems [48].

### 2.2.3.2 FMN Domain

The FMN domain, consisting of residues from 67 to 231 of rat POR, is structurally very similar to the bacterial flavodoxins and consists of a five-stranded parallel  $\beta$ -sheet flanked by five  $\alpha$ -helices (Fig. 2.2), with the FMN located at the tip of the C-terminal side of the  $\beta$ -sheet. In addition to the binding site for the FMN prosthetic group, this domain contains residues mediating binding of and electron transfer to acceptors such as *cyt c* and P450. FMN is relatively loosely bound ( $K_d \sim 10^{-8}$  M) and can be reversibly removed from the enzyme by high salt treatment [27, 49]. In the absence of FMN, electron transfer to all acceptors, with the exception of ferricyanide, is abolished.

As observed in Fld, the isoalloxazine ring of FMN is sandwiched between two aromatic groups with Tyr178 coplanar with the *si*-face of the flavin, and Tyr140 located on the *re*-face at a  $\sim 60^\circ$  angle to the isoalloxazine ring [36]. Mutation of Tyr178 to Asp decreases FMN binding to undetectable levels, with an approximately 300-fold decrease in FMN binding affinity, and also disrupts FAD binding [50]. A similar decrease in FMN binding affinity is seen when the homologous residue of human POR, Tyr181, is mutated to Asp [51, 52]; however, FAD binding is not disrupted in the case of the human mutation. Restoration of catalytic activity by FMN demonstrates that the inability to incorporate FMN is the likely basis for the NADPH-cytochrome P450 oxidoreductase deficiency (PORD) phenotype associated with this human mutation. The rate of electron transfer to ferricyanide activity is identical to that seen in the wild-type enzyme, indicating that the hydride transfer is not impaired.

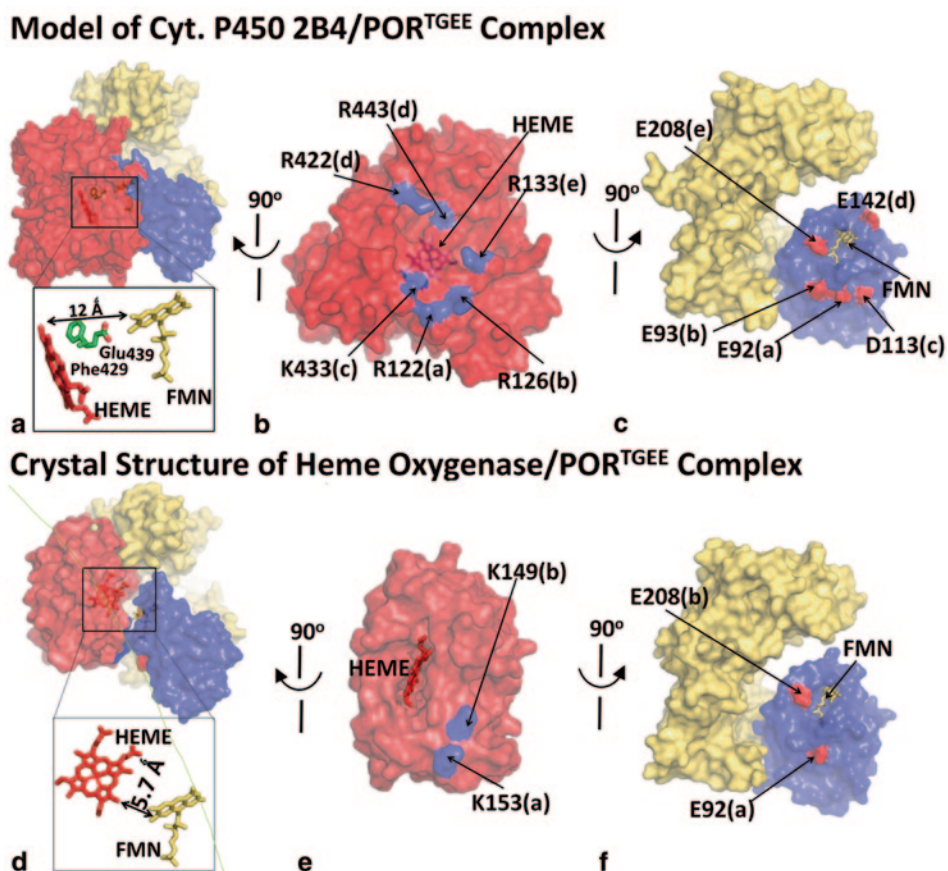


**Fig. 2.5** *Top panel:* **a** Model of a complex between P450 and NADPH-cytochrome P450 oxidoreductase (POR). A complex of P450 (red) and Mol A of the hinge-deletion mutant of POR( $\Delta$ TGEE), denoted as POR<sup>TGEE</sup> [53]; the flavin mononucleotide (FMN) domain (blue) and flavin adenine dinucleotide (FAD) domain (yellow)] and an enlarged view showing the relative orientation of the FMN and heme. **b** and **c** Open-book representation of molecular surface at the interface of P450 (**b**) and the FMN domain of POR (**c**). Five salt-bridge pairs are shown with same let-

ters, e.g., Glu142(d) makes salt bridges with both Arg422 (d) and Arg443 (d). *Bottom:* **d** Crystal structure of the complex between POR( $\Delta$ TGEE) and heme oxygenase-1 (HO-1). **e** and **f** An open book representation, showing the interface between the two partners. Two salt-bridge pairs are shown. The surface of  $\Delta$ TGEE that interacts with HO-1 (*Panel F*) is almost the same interface found in the model structure of POR-2B4 (*compare Panels C and F*). The structure of the POR( $\Delta$ TGEE)-HO-1 complex supports the validity of the model structure of POR-P450 2B4.

### 2.2.3.3 Role of the FMN Domain and Connecting Domain in the Cytochrome P450 Interaction

The negatively charged surface of the FMN domain can interact with the basic concave proximal face of P450 in the vicinity of the buried heme ligand [53–56]. This region of P450 contains overlapping binding sites for POR and cyt *b*<sub>5</sub> [54]. A model of a putative complex of P450 2B4 and POR shows the total contact area between the two molecules to be  $\sim 1500 \text{ \AA}^2$ , of which  $870 \text{ \AA}^2$

is located between the FMN domain and P450 [53]. A number of charge pairing and van der Waal's interactions have been implicated in binding of P450 to POR, indicating that both electrostatic and hydrophobic interactions are necessary for the complex formation (Fig. 2.5).

The FMN domain has conserved patches of acidic residues involved in the electrostatic interactions with its electron transfer partners, and these interactions are specific for each electron transfer partner. Cross-linking experiments

suggest that acidic residues in the FMN domain (<sup>207</sup>Asp-Asp-Asp<sup>209</sup> and <sup>213</sup>Glu-Glu-Asp<sup>215</sup>) contribute to binding of cyt *c*; however, cross-linking of these residues to P450 could not be demonstrated [57, 58]. Mutagenesis studies have demonstrated the importance of Glu213 and Glu214 in electrostatic interactions with oxidized and reduced cyt *c*. The <sup>213</sup>Glu-Glu-Asp<sup>215</sup> cluster does not affect P450 binding or activity, highlighting the distinct binding modes for these two partners [59]. Chemical modification and antibody labeling experiments have also suggested that the loop containing residues 110–119 in POR, located on the opposite face of the protein, can also contribute to P450 binding and catalysis (reviewed in [60]). Site-directed mutagenesis of Asp113, Glu115, and Glu116 improves catalytic efficiency of cyt *c* reduction, but destabilizes the POR-CYP2B1 complex [61]. A variety of chemical modification and mutagenesis studies, reviewed by Hlavica et al. [62] and Im and Waskell [55], have provided evidence implicating basic residues in the C-helix of P450 in electrostatic interactions with POR and cyt *b*<sub>5</sub>. Site-directed mutagenesis studies have identified seven basic and hydrophobic amino acids (Arg122, Arg126, Arg133, Phe135, Met137, Lys139, and Lys433), all except Lys433 located in the mobile C-helix and C–D loop, as important for both cyt *b*<sub>5</sub> and POR binding [54]. Mutations to proline of residues in the linker between the two flavin domains also increased the cyt *c* reduction activity, presumably by favoring the open conformation of POR [63]. The hydrophobic amino acid residues Val267 and Leu270 on the proximal site of CYP2B4 also contribute to POR recognition, perhaps indirectly through a conformational change [64]. Although the electron transfer is presumed to occur within a 1:1 POR:P450 complex [65], the presence of higher-order complexes contributing to catalysis has been suggested [23, 66, 67]. The contribution of these higher-order complexes to catalysis in microsomes is not clear. However, it is likely that multiple P450s may associate to POR during the selection process in the course of catalysis as an encounter complex (see Sect. 2.3.2).

### 2.2.3.4 The FAD Domain

The FAD domain of POR is composed of the connecting domain (CD) and the FNR-like subdomain, which binds FAD and NADPH (Figs. 2.1 and 2.2). The FNR-like subdomain sequence consists of residues 267–325 and 450–678, interspersed with the CD (residues 244–266 and 326–450). Conserved residues necessary for FAD and NADPH binding, as well as for hydride transfer, are localized in this FNR-like subdomain. Unlike FMN, FAD is tightly bound to the reductase with a *K*<sub>d</sub> less than 1 nM. Removal of FAD requires treatment with a high concentration of chaotropic agent that leads to substantial polypeptide unfolding, providing further evidence for the independence of the two domains [68–70]. Residues comprising the FAD binding site include <sup>455</sup>YYSIASS<sup>461</sup>, <sup>471</sup>ICAVAVEY<sup>478</sup>, and <sup>488</sup>GVAT<sup>491</sup>. Although Trp677 is stacked against the *re*-face of the FAD, removal of this residue does not have a significant effect on FAD content; the role of this residue in catalysis is discussed below. Major determinants of FAD binding are Arg454, which stabilizes the negative charge of the FAD pyrophosphate, and Tyr456, which is positioned at a 60° angle to the *si*-face of the isoalloxazine ring and whose phenolic hydroxyl group forms a hydrogen bond with the ribityl 4'-hydroxyl [36, 71]. An unexpected finding for residues that influence FAD-binding was revealed in a human pathogenic mutant, Val-492Glu (rat enzyme numbering, V489), which has less than 1% of wild-type FAD content (see Sect. 2.6).

## 2.2.4 Mechanism of Catalytic Action

### 2.2.4.1 Hydride Transfer

POR transfers the *pro-R* hydrogen from NADPH to FAD as a hydride ion. Residues essential for this hydride transfer include Ser457, Asp675, and Cys630, all of which are located in close proximity to the redox-active N5 of FAD and form a hydrogen bonding network that is disrupted upon



binding of the nicotinamide moiety of NADP(H) [72–74]. Replacement of these side chains with aliphatic groups decreases catalytic activities by up to three orders of magnitude. Ser457 and Asp675 interact with the nicotinamide group of NADP(H) and orient the C4 atom of the nicotinamide ring in a position for optimum hydride transfer. Cys630 is also within van der Waals distance from the nicotinamide C4 and can stabilize the carbocation formed during hydride transfer [74]. In addition, the hydroxyl side chain of Ser457 is located  $\sim 4 \text{ \AA}$  away from the flavin N5 and on the same plane as the flavin ring, in a position to stabilize the semiquinone form of FAD, and replacement of Ser457 with alanine decreases the FAD/FADH• redox potential [72].

The penultimate Trp677 residue plays a pivotal role in catalysis by controlling NADP(H) binding and release [74]. In the structure of the wild-type reductase in complex with NADP<sup>+</sup>, the indole ring of Trp677 is situated at the *re*-face of the FAD, where the nicotinamide ring of NADPH would bind to transfer its *pro*-R-hydrogen as a hydride ion. Furthermore, in the structure of the wild-type enzyme, the binding site for the AMP-pyrophosphate half of the NADP<sup>+</sup> is clearly shown, while the ribose-nicotinamide moiety is disordered. However, crystal structures of a POR mutant lacking the indole ring by deletion of the two last C-terminal residues (Trp677 and Ser678), or mutation of Trp677 to glycine (Trp677Gly), reveal that the nicotinamide ring is situated at the *re*-face of the FAD, replacing the indole ring of Trp677, with a tilt of  $\sim 30^\circ$  between the planes of the two rings, poised to transfer the hydride ion [74]. Thus, in the wild-type protein, the indole ring of Trp677 presumably moves away from the isoalloxazine ring of FAD, allowing the nicotinamide ring to interact with the flavin for hydride transfer to occur. In pea FNR, the homologous residue, Tyr308, is also displaced by the nicotinamide ring [75, 76].

Mutagenesis and crystallographic studies have revealed the bipartite nature of NADP(H) binding and provide an explanation of the marked preference of POR and FNR for the cofactor NADPH. The primary determinant for discrimination between NADH and NADPH is the 2'-phosphate group present on NADPH,

but not NADH. Kinetic studies show that this 2'-phosphate of NADPH, binding as the dianion, contributes 5 kcal of binding energy through interactions with enzyme groups, with a major contribution with Arg597 accounting for  $\sim 3$  kcal of binding energy. Lys602 and Ser596 also contribute to binding [77]. This tight binding of the 2'-phosphate is essential to compensate for the repulsive interactions between the nicotinamide and the indole ring of Trp677. When Trp677 is present, binding of the 2'-phosphate stabilizes cofactor binding sufficiently to allow the nicotinamide to displace Trp677. In the absence of Trp677, the nicotinamide can bind readily without any contribution from the 2'-phosphate and the enzyme is able to utilize NADH as the hydride donor. Furthermore, in the absence of Trp677, the enzyme is unable to displace oxidized nicotinamide after hydride transfer and catalytic efficiency with either NADH or NADPH is decreased due to rate-limiting product release [74, 78, 79], indicating that movement of Trp677 is required for both cofactor binding and release.

These studies indicate a requirement for structural changes, in addition to Trp677 movement, for regulation of NADP(H) binding and release. While movement of Trp677 back into the nicotinamide binding site (*re*-face of the FAD isoalloxazine ring) displaces the nicotinamide ring, additional movements are necessary to disrupt the strong binding of the 2'-phosphate. Local movements of the <sup>631</sup>GDAR<sup>634</sup> loop (Asp632 loop), located near the FAD, may be coupled with Trp677 movement to allow NADPH binding and NADP<sup>+</sup> release [80]. Comparison of the structure of the NADP<sup>+</sup>-bound wild-type enzyme with that of a mutant POR with an engineered disulfide bond between the two flavin domains and lacking bound NADP<sup>+</sup>, shows a movement of this Asp632 loop. Thus, Xia et al. have proposed that Asp632 loop movement, in concert with Trp677, controls at least in part NADPH binding and NADP<sup>+</sup> release [80], and the details are discussed below in Sect. 2.5.

#### 2.2.4.2 Interflavin Electron Transfer

POR intramolecular electron transfer occurs directly from FAD to FMN. In rat and human POR [36, 81], the distance between the

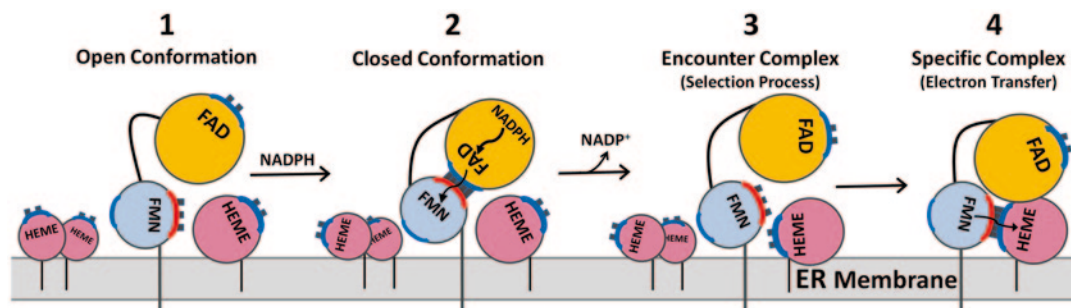


**Fig. 2.6** A cartoon representation of a model for POR-P450 complex formation in the endoplasmic reticulum (ER) membrane. Flavin mononucleotide (FMN) domain, flavin adenine dinucleotide (FAD) domain, and P450s are shown in blue, yellow, and red balls, respectively. (1) Multiple P450s exist in the ER membrane. Nucleotide binding favors formation of the closed form, similar to the one found in the crystal structure [36]. (2) Upon binding to pyridine nucleotide (NADPH), the enzyme adopts the closed form. In the closed form, hydride transfer, inter-

dimethylbenzene edge of the isoalloxazine rings of FAD and FMN is  $\sim 4 \text{ \AA}$ , and the planes of the FAD and FMN rings are inclined relative to each other at an angle of  $\sim 150^\circ$ , an orientation that favors orbital overlap between the extended  $\pi$ - $\pi$  systems of the flavin isoalloxazine rings [74]. This arrangement of the two flavins is expected to result in very fast and efficient interflavin electron transfer, up to  $10^{10} \text{ s}^{-1}$  using Dutton's ruler [82]. However, the experimentally observed electron transfer rate has been measured to be only  $\sim 50 \text{ s}^{-1}$  [83, 84], suggesting that electron transfer is gated by some other process. The nature of the conformational movements controlling the rates of interflavin as well as flavin to heme electron transfer is discussed below.

#### 2.2.4.3 Electron Transfer from FMN to Heme

The FMN domain functions both to accept electrons from the reduced FAD and to transfer those electrons to P450. Thus, precise and specific interactions between the FMN and FAD domains within POR, and between the FMN domain and P450 are required. This means that the FMN domain must be able to recognize both the FAD domain and P450. Separation of the two flavin domains is essential for this sequential electron transfer process. The FMN domain has a strong

flavin electron transfer, and release of NADP<sup>+</sup> occur, resulting in formation of the open form of the enzyme. (A scheme for detailed conformational changes occurring during this process is shown in Fig. 2.7.) (3) The open form of POR associates with P450 in an encounter complex. (4) Further conformational adjustments occur to align the flavin and heme groups in an optimal conformation for electron transfer, and the cycle repeats. (Figure adopted and modified from [86])

molecular dipole formed by anionic residues surrounding the flavin isoalloxazine ring [85]. This convex anionic surface is involved in the specific docking with the heme protein. Little is known about the mechanism through which POR selects one of many electron transfer partners and it is likely that multiple protein conformations and binding sites are probed in the selection process. Figure 2.6 presents a scheme incorporating current hypotheses regarding formation of a productive POR-P450 electron transfer complex. Beginning from a pool of P450s in the ER membrane, in which multiple P450s exist, a selection process must occur by which one P450 binds in a more favorable conformation. A proposed sequence of events is as follows: (1) NADPH binds to the open form of POR, resulting in a closed conformation of POR. (2) In this closed conformation, hydride transfer and interflavin electron transfer occur, followed by NADP<sup>+</sup> release, resulting in an open conformation of POR. (3) This open form of POR is now capable of forming an eventual productive complex. It should also be noted that POR will favor substrate-bound ferric P450s compared to substrate-free P450s. Substrate binding increases the redox potential of the P450, makes the electron transfer reaction thermodynamically feasible, and prevents inappropriate reduc-

tion of P450. Substrate binding may also induce conformational changes on the proximal surface that favors POR binding. (4) A loosely bound encounter complex is formed [87]. (5) Further conformational changes at the interface are necessary to produce the electron transfer complex, in which the flavin and heme are appropriately positioned for electron transfer [87]. For a more detailed discussion on general protein–protein interactions, see the latter part of this chapter. The requirements for cyt *c* binding are most likely less stringent than those for P450, and kinetic studies suggest the presence of more than one binding site for cyt *c* [88]. In contrast, the mechanism of electron transfer to small molecule acceptors such as dichloroindophenol or ferricyanide presumably involves random collisions followed by electron transfer.

A model for a docked POR-P450 complex (POR-P450 2B4) based on mutagenesis data with the open conformation of the POR hinge mutant (four amino acid deletion in the hinge between two flavin domains) by Hamdane et al. [53] indicates that the FMN domain interacts with the concave basic proximal face of P450. The planes of the heme and FMN are almost perpendicular to each other, and the shortest distance between the heme and flavin cofactors is about 12 Å (Fig. 2.5). However, two residues of P450 2B4, Phe429, and Glu439, lie in between the two cofactors, suggesting that these might serve to facilitate electron transfer between the FMN and heme. In the structure of the complex between the heme and FMN-binding domains of bacterial cytochrome P450BM3, the relative orientation of the two cofactors is similar to that found in the model structure, but the distance between the FMN and heme is slightly longer (~18 Å) [89], indicating the validity of the model structure. Recently, the crystal structure of the complex between the four-residue hinge deletion mutant of POR ( $\Delta$ TGEE) and rat heme oxygenase 1 (HO-1) has been determined [90]. The complex structure reveals that the distance between FMN and the heme is ~6 Å. However, the surface of  $\Delta$ TGEE that interact with HO-1 is almost identical to that found in the model structure of POR-2B4, although the interface area is smaller, since HO-1

is a smaller molecule than P450 (Fig. 2.5). This finding is consistent with the argument that the model structure of the POR-P450 2B4 complex is an appropriate initial model for further experimental design.

## 2.2.5 Domain Movement and Electron Transfer in POR

As stated above, the relatively slow rate of interflavin electron transfer suggests a gating mechanism. Crystal structures of various POR proteins, including the rat [36], human [81], and yeast PORs [91], and their various mutant proteins [74], clearly demonstrate that the enzyme molecule consists of two flavin-binding domains, and that the two cofactors are juxtaposed to each other with their dimethyl benzene rings facing one another, with the closest distance being ~4 Å. Although this arrangement of the two flavin domains (“closed” conformation) is optimal for electron transfer between the two flavins, i.e., from FAD to FMN, it is incompatible with interaction of the FMN domain with P450, the physiological electron acceptor. In the closed conformation, the acidic residues located in the FMN domain and shown to affect electron transfer to P450 by mutagenesis studies [59] are not exposed to solvent, and therefore cannot interact with P450. In addition, the crystal structure of a complex between the heme and FMN-binding domains of P450BM3 provides structural insight into how these two domains interact with each other [89]. In this structure, the FMN dimethylbenzene ring is oriented toward the proximal face of the heme of P450 BM3, suggesting that POR must interact with P450 in a different conformation than the closed conformation observed in the wild-type POR crystal structure.

There are several lines of evidence from crystallographic studies, demonstrating that the two flavin domains are mobile. Superposition of the structures of wild-type and various point mutant structures of rat POR has shown that the relative orientation of, and distance between, the two flavin domains are variable, with the closest flavin–flavin distance ranging from 3.9 to

5.8 Å, suggesting small, but significant domain movements in solution [74]. Moreover, in the crystal structure of the flavoprotein subunit of *E. coli* sulfite reductase, electron density for the entire FMN domain is completely disordered, again suggesting movement of the FMN domain relative to the rest of the polypeptide [92]. The most direct demonstration of a large-scale domain movement and a transition from a closed to an open conformation comes from the crystal structures of mutant POR proteins. A POR variant with a four amino acid deletion in the hinge region that links the two flavin domains has been crystallized in three different extended conformations (open state), in which the distance between FAD and FMN cofactors ranges from 30 to 60 Å [53]. The mutant is defective in its ability to transfer electrons from FAD to FMN. However, when FMN is reduced chemically, the mutant POR is capable of reducing P450 2B4. The authors infer that a similar domain movement controlled by the hinge occurs in the wild-type enzyme during its catalytic cycle, enabling the FMN domain to adopt an open conformation capable of interacting with its physiological partner, cytochrome P450. Aigrain et al. have also seen an open conformation in the crystal structure of a yeast-human chimeric POR [93]. A different, but complementary approach has been used by Xia et al. [80], in which an engineered disulfide linkage between the two flavin domains locks POR in a closed conformation unable to interact with P450. Indeed, the mutant exhibits substantially decreased inter flavin electron transfer and is essentially unable to catalyze the P450-dependent monooxygenase activity. Reduction of the disulfide linkage restores the ability of the mutant to support both interflavin electron transfer and reduction of its redox partners, consistent with domain movements being required for the FMN domain of POR to interact with both the FAD domain and P450, i.e., shuttling between the two redox-active partners.

In addition, several solution studies provide evidence for large domain movements of POR in catalysis. Hay et al., demonstrate, using electron-electron double resonance methods, that POR exists in multiple conformations in a continuum

of a conformational landscape that is changed by nucleotide binding [94]. Using a combination of nuclear magnetic resonance (NMR) and small-angle X-ray scattering (SAXS) methods, Ellis et al. [95] have shown that the oxidized human POR exists in solution as a mixture of approximately equal amounts of two conformations, one consistent with the crystal structure (closed form) and one a more extended structure, which presumably is required for interaction with its electron transfer partners (open form). In addition, the relative contributions of each conformation at equilibrium are affected by the binding of NADP(H), with the nucleotide bound form favoring the closed form. On the other hand, Vincent et al. [96] have recently employed high resolution NMR measurements with residue-specific  $^{15}\text{N}$  relaxation and  $^1\text{H}$ - $^{15}\text{N}$  residual dipolar coupling data to show that oxidized POR in solution in the absence of bound nucleotide exists in a unique and predominant conformation resembling the closed conformation observed in the crystal structure. However, at present more data are accumulating for the predominance of the closed form when the nucleotide is bound. Pudney et al. [97] have demonstrated, using a combination of fluorescence resonance energy transfer and stopped flow methods, that open and closed states of POR are correlated with key steps in the catalytic cycle, i.e., NADPH binding induces closing of POR and reduction of flavins and/or  $\text{NADP}^+$  release induces opening of POR. Recently, Huang et al. have shown, using small angle X-ray scattering and small angle neutron scattering together with site-directed mutagenesis, that POR in solution exists in equilibrium between a compact (closed) conformation and an extended (open) conformation and that this equilibrium is linked to nucleotide binding and redox state [63]. Currently, it is generally agreed that the closed conformation is favored when the NADP(H) is bound and the FAD is oxidized; and that the enzyme adopts an open conformation ready to transfer electrons to P450, i.e., when the enzyme is reduced and  $\text{NADP}^+$  has been released (see Fig. 2.6).

In summary, there is mounting evidence that POR must undergo several different types of

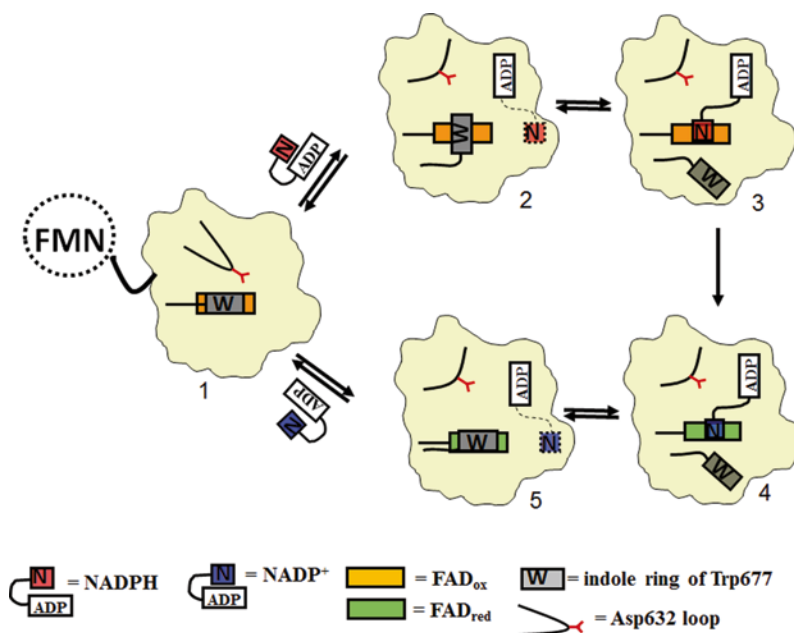


**Fig. 2.7** Schematic illustration of conformational changes occurring in the flavin adenine dinucleotide (*FAD*) domain upon NADPH binding to and NADP<sup>+</sup> release from NADPH-cytochrome P450 oxidoreductase (*POR*). *Stage 1*: NADPH enters oxidized *POR* (modeled after the structure of the disulfide cross-linked mutant, which lacks bound NADP(H)) [80]. The open-closed state of *POR* at this stage is not known, but is most likely in an open form. Stages 2–5 are most likely in the closed form. Therefore, for clarity, the flavin mononucleotide (*FMN*) domain is not shown. *Stage 2*: NADPH initially binds to the enzyme via its AMP-PP<sub>i</sub> moiety with the interaction between the negative charges of pyrophosphate and 2'-phosphate with the positive charges of several arginine residues in the binding pocket (see text). As the AMP-PP<sub>i</sub> half of NADPH binds, and the Asp632 loop moves, allowing the ribose–nicotinamide moiety to extend to search for the proper binding site for hydride transfer, while keeping

the AMP-PP<sub>i</sub> anchored. At this stage, the indole ring of Trp677 also rotates to be ready to move away from the flavin ring. *Stage 3*: The indole ring moves away to make room for the nicotinamide ring to bind, as the nicotinamide ring moves in at the *re*-side of the isoalloxazine ring. *Stage 4*: Hydride transfer occurs, FAD is reduced, and NADPH becomes NADP<sup>+</sup>. It is most likely that interflavin electron transfer occurs at this stage. *Stage 5*: Once the FAD is reduced and nicotinamide is oxidized, the oxidized nicotinamide ring moves out, with the concomitant return of the indole ring to the *re*-face of the FAD ring. At this stage, the Asp632 loop moves back closer to where the AMP-PP<sub>i</sub> of NADP<sup>+</sup> lies, causing steric hindrance as well as electrostatic repulsion, resulting in dissociation of the cofactor from the enzyme. *POR* now returns to stage 1 and the cycle repeats. (Figure adopted and modified from [80])

conformational changes during catalysis. Hubbard et al. have shown that, upon binding of NADPH, the C-terminus of *POR* including the aromatic residue Trp677 undergo significant conformational changes [74]. In addition, comparison of the structure of *POR* with and without bound NADP<sup>+</sup> suggests that the movement of the loop containing Asp632 is necessary for binding of the nicotinamide moiety of NADPH to the *re*-face of the FAD isoalloxazine ring. Given these results, suggesting that Trp677 and the Asp632 loop movements occur together, Xia et al. [80] have proposed a scenario for coordinated con-

formational changes that occur during NADPH binding, hydride transfer and NADP<sup>+</sup> release (Fig. 2.7). Since NADPH-binding and Trp677 movement precede hydride transfer, these steps and the subsequent interflavin electron transfer step must occur with the enzyme in the closed conformation. This is followed by a large-scale domain movement to the open conformation that is necessary for interaction with P450. This large movement must be tightly coordinated with electron transfer to prevent reactions with oxygen and production of superoxide. It is most likely that a similar sequence of conformational changes

would also take place in other members of the diflavin oxidoreductase family. However, details of the mechanism by which the large-scale domain movements are coordinated to movements of loops and individual amino acids remain to be established. Furthermore, at this time it is unknown whether stochastic domain movements play a role in the mechanism of action of POR or whether they are strictly controlled.

### 2.2.6 Human POR Deficiency

Several lines of evidence exist in different biological systems demonstrating the essential cellular functions of POR-dependent P450 activity. The entire POR gene deletion is lethal in yeast and *Caenorhabditis elegans* due to impaired P450-dependent biosynthesis of ergosterol and an as-yet unidentified lipid, respectively [98–100]. Global deletion of murine microsomal POR produces multiple developmental defects and embryonic lethality. Neural tube, cardiac, eye, limb, and vascular defects are seen in homozygous null embryos, as well as a failure of development, which have been ascribed to defects in cholesterol and retinoid metabolism [101, 102].

The ability to delete POR in a tissue-specific manner has provided further insights into the diverse physiological functions of POR, both in metabolism of endogenous substrates and xenobiotic metabolism. Liver-specific ablation of *POR* gave rise to massive lipid accumulation and hepatomegaly, in the presence of decreased serum cholesterol and triglyceride levels, suggestive of defects in regulation of hepatic lipid metabolism. Consistent with the central role of hepatic POR in drug metabolism, liver-specific ablation of POR decreased metabolism and/or clearance of xenobiotics [103–106]. Current developments of various mouse models were presented at a symposium in Experimental Biology 2012 (Symposium Report published [107]).

Since the first report of four individuals with POR deficiency [108], numerous reports worldwide have been published, describing the varying phenotypes associated with this syndrome. A total of over 2000 single nucleotide polymorphisms

have been described in the human POR gene ([www.ncbi.nlm.nih.gov/snp](http://www.ncbi.nlm.nih.gov/snp)), encompassing over 150 missense mutations (including premature terminations), over 10 frame shift/deletion/duplication mutations, and 9 splice site variants. Mutations affecting transcription have also been identified and interpreted in terms of the POR promoter structure [109, 110]. Detailed information on POR deficiency with a clinical focus can be found in several excellent reviews [111–113].

Mutations in human POR that significantly disrupt cholesterol biosynthesis and/or steroidogenesis have been shown to result in POR deficiency, characterized by Antley–Bixler syndrome and disordered steroidogenesis [108, 114]. Clinical findings vary greatly in POR deficiency, ranging from severe skeletal malformations associated with the Antley–Bixler syndrome and congenital adrenal hyperplasia to relatively mild hormonal dysregulation. In general, the most severe phenotypes are associated with largest disruptions in ability of POR to support P450-dependent activity [112]. CYP17A1 is known to be particularly sensitive to perturbations in electron transfer, with 17,20 lyase activity favored over 17 $\alpha$  hydroxylase activity in the presence of cyt *b*<sub>5</sub> [116]. Therefore, disordered steroidogenesis is a prominent feature of POR deficiency, which distinguishes it from the Antley–Bixler syndrome with normal steroidogenesis associated with mutations in the fibroblast growth factor receptor 2 (FGFR2) gene. POR deficiency is also associated with congenital adrenal hyperplasia without Antley–Bixler abnormalities. However, recent studies show that conditional deletion of the POR gene in osteoprogenitor cells affects long bone and skull development in mice, recapitulating Antley–Bixler syndrome [117]. These results also suggest an apparent link between the POR and FGFR signaling pathways.

Sequence homology and mapping of missense mutations onto the POR crystal structure have allowed identification of the functions of several missense mutations. Tyr181Asp, Arg457His, Tyr459His and Val492Glu mutations result in low cyt *c* and CYP17A1 activities; Tyr181Asp causes decreased affinity for FMN-binding [51,

118], and Arg457His and Val492Glu cause decreased FAD-binding affinity [108, 119]. The results of Tyr181Asp and Tyr459His mutations are entirely consistent with the hypothesis that the aromatic residues are required for binding of FAD and FMN [81, 119]. Furthermore, the crystal structures of human wild-type and two variants (Val492Glu and Arg457His) have been determined [81]. The overall 3D structures of Arg457His and Val492Glu variants are similar to wild-type; however, there are subtle, but significant differences, including local disruption of hydrogen bonding and salt bridging involving the FAD pyrophosphate moiety, leading to weaker FAD binding, an unstable protein, and loss of catalytic activity, all of which can be rescued by cofactor addition. Thus, riboflavin therapy may prevent or rescue from POR dysfunction patients with these mutations [81, 119].

Although mutations that dramatically decrease POR activity are rare, other polymorphisms, such as Ala503Val, are quite common and there is interest in the effects of these variations on inter-individual variability in drug metabolism [120–122]. The complexity of this effort may be illustrated by studies on the Ala503Val mutant, which has an allele frequency of ~27% [120–122]. In view of the high frequency of this allele, several studies have attempted to assess the contribution of this mutation to inter-individual variation in drug metabolism. Variable results are reported, depending on the P450, the substrate, and the assay systems employed [123–126]. It is increasingly apparent that the effects of POR variants on P450-mediated metabolism require examination of each P450-POR pair and possibly each substrate separately, with further complications introduced by the membrane environment.

## 2.3 Interaction Between Cytochrome $b_5$ and Cytochrome P450

### 2.3.1 Properties of Cytochrome $b_5$

Cytochrome  $b_5$  (cyt  $b_5$ ) is a 134 amino acid membrane-bound electron transfer heme protein that is anchored to the ER membrane by its COOH

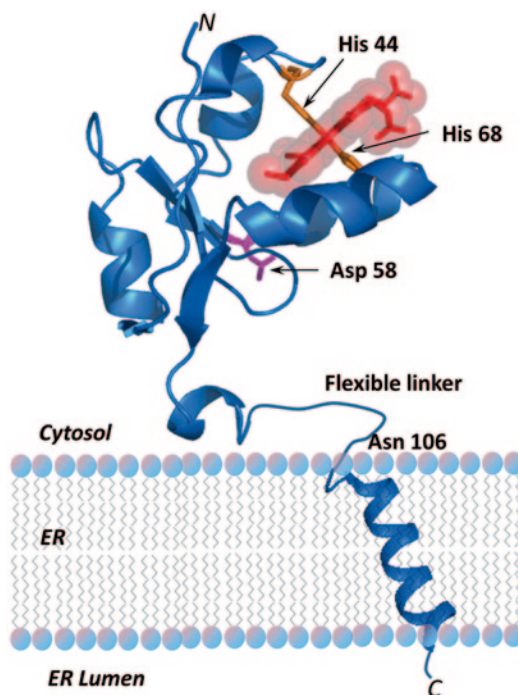


**Fig. 2.8** Structure of the heme domain and flexible linker of cyt  $b_5$  and a model of the transmembrane domain in a bilayer

terminus. The soluble heme domain and membrane anchor are connected by a ~14 amino acid random coil linker [54, 127–129] (Fig. 2.8). It also exists as a soluble protein in red blood cells, where it transfers electrons from cyt  $b_5$  reductase to hemoglobin. Its membrane-bound form provides electrons for the biosynthesis of lipids including plasmalogens, cholesterol, and long-chain fatty acid desaturation [127, 129]. In these reactions, cyt  $b_5$  reductase provides the electrons to cyt  $b_5$ . A cyt  $b_5$  domain also exists as a fusion protein in mitochondrial sulfite oxidase,  $\Delta 5$ - and  $-\Delta 6$  fatty acid desaturases in animals, yeast inositol phosphorylceramide oxidase, plant nitrate reductase,  $\Delta 9$ -fatty acid desaturases in baker's yeast, NADH cyt  $b_5$  oxidoreductase in animals, and flavocytochrome  $b_2$  in yeast mitochondria [127, 130]. A closely related mitochondrial cyt  $b_5$  has also been described. The human mitochondrial cyt  $b_5$  has been shown to provide electrons to an amidoxime-reducing electron transfer chain. It reduces a molybdenum containing enzyme,

which, in turn, directly reduces the N-hydroxylated substrate [131].

The interaction of cyt  $b_5$  and P450 has been well established. However, it remains a complex and controversial topic that has been reviewed previously [54, 127, 132]. In vitro in reconstituted systems, as well as in vivo in the mouse knockout and the mouse with a conditional hepatic deletion of cyt  $b_5$ , the effects of cyt  $b_5$  on P450 are contradictory and incompletely understood [132–136]. In purified reconstituted systems, cyt  $b_5$  has been observed to stimulate the activity of some P450s (CYP2B4, CYP2E1, CYP2B1, CYP4A7, CYP2A6, CYP2C19, CYP3A4, CYP17A). In contrast, cyt  $b_5$  has no significant effects on the activity of P4501A2 and 2D6 [137]. Reports have also appeared of inhibition of P450 activity by cyt  $b_5$  [132, 138, 139]. In vivo disposition of drugs in the total body cyt  $b_5$  knockout mouse and in the conditional hepatic cyt  $b_5$  deletion mouse were also complex. The metabolism of some drugs was decreased, while degradation of other drugs was not affected [136, 140]. This chapter will primarily emphasize advances in our understanding of the P450-cyt  $b_5$  interaction that have occurred over the past decade. More than four decades ago, it was shown that cyt  $b_5$  had the ability to decrease the concentration of oxy  $\text{Fe}^{+2}$  P450 in hepatic microsomes upon addition of NADH to an NADPH-containing reaction mixture, which was consistent with the ability of cyt  $b_5$  to transfer electrons to P450. The molecular basis of this interaction between cyt  $b_5$  and P450 has intrigued investigators ever since [141].

### 2.3.2 General Characteristics of Interprotein Interactions

Before proceeding with the specifics of the P450-cyt  $b_5$  interaction, the properties of interprotein interactions in general will be presented to provide the framework for the discussion of the P450-cyt  $b_5$  interaction and to help appreciate the P450-POR interaction discussed in the previous section of this chapter. In order for electron transfer to occur between proteins, they must come into contact [142]. Complexes formed between

electron transfer proteins typically are weak, on the order of millimolar to micromolar affinities [143]. This weak affinity allows specific but not too perfect binding, so that redox partners can bind, but then readily dissociate and proceed to recycle. If proteins were free in solution, a collision would require a 3D search for the electron transfer site. However, in redox proteins and many other protein complexes, the docking sites have been designed to increase the efficiency of the interaction by employing electrostatic steering and structural complementarity. Electrostatic forces are inversely proportional to the square of the distance between the charged surfaces and are effective over distances up to 25 Å. Structural complementarity is also a major driving force for protein binding. In the case of P450 and its redox partners, cyt  $b_5$  and P450 reductase, the binding of the proteins to the membrane is also hypothesized to decrease the search for the docking site from three to two dimensions. Although electrostatic forces enhance the association rate of proteins, they are considered to result in an “encounter complex,” which may not be the optimal electron transfer complex. Following formation of the “encounter complex,” short-range diffusion occurs at the interface with sidechains and backbone atoms of residues at the interface undergoing rapid motions to identify a suitable electron transfer complex [87]. Electron transfer occurs rapidly over distances of 14 Å or less, thereby assuring that electron transfer is faster than the usual millisecond bond-breaking at the catalytic site [142]. The 14 Å distance is between the edges of the entities, such as heme and the isoalloxazine ring, exchanging electrons. Quantum chemical calculations suggest that the wave function of a free electron localized at a redox center, for example heme, extends beyond the cofactor in all directions, while decaying exponentially into the electrically insulating amino acid medium [144]. To maintain charge neutrality, proton transfer often occurs essentially simultaneously with electron transfer.

Clackson and Wells have shown that an average of 10–30 residues from each protein are in contact in crystal and NMR structures at an interprotein interface, but that only three to four



amino acid pairs contribute the majority of binding energy to the complex [145]. Site-directed mutagenesis is the major tool employed to investigate which amino acids are most critical. Often, the key residues are found near the center of the interface while the more peripheral residues contribute less binding energy to complex formation, but most likely serve to occlude bulk solvent from the hot spot. Hydrophobic and ionic interactions, as well as hydrogen bonds, are all typically found in a protein interface, although one type of interaction may dominate [146]. It has also been noted that redox proteins that are reactive toward multiple partners, such as *cyt*  $b_5$  and P450 reductase, employ binding sites that are able to accommodate a variety of molecular surfaces [147].

### 2.3.3 Interactions Between Cytochrome $b_5$ and Cytochrome P450

Bearing in mind the preceding brief background about the nature of typical interprotein interactions, the specifics of the P450-*cyt*  $b_5$  interaction will be discussed. Figure 2.9 is a schematic of the reaction cycle of P450 with *cyt*  $b_5$  and P450 reductase. As a result of the demonstration in hepatic microsomes: (1) that *cyt*  $b_5$ , which has been reduced by NADH, was partially oxidized upon addition of NADPH when substrate and oxygen were present and (2) that it coincided with product formation, it was hypothesized that *cyt*  $b_5$  donated an electron to oxyferrous P450. This suggestion was consistent with two observations. One was that, under steady-state conditions in microsomes, the absorbance of oxyferrous P450 at 440 nm decreased in the presence of NADH [141]. A second observation was that NADH enhanced NADPH-supported catalysis in microsomes. Both experiments contributed support to the notion that *cyt*  $b_5$  was able to provide the second electron required for P450 catalysis [148].

These reports have prompted the performance of a large number of experiments over the ensuing decades by a number of investigators in an attempt to understand how *cyt*  $b_5$  enhanced catalysis in hepatic microsomes and why POR was

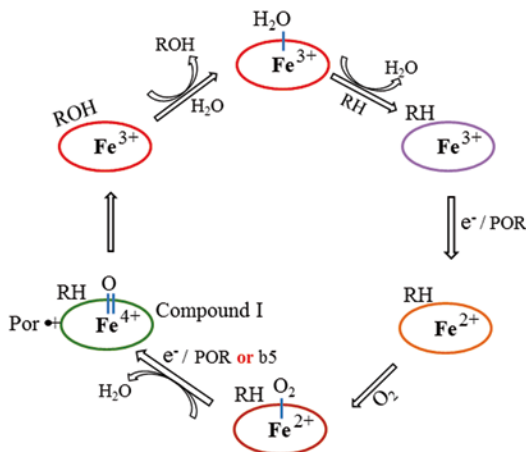


**Fig. 2.9** A scheme of the P450 reaction cycle, including interactions with its redox partners, NADPH-cytochrome P450 oxidoreductase (POR) and *cyt*  $b_5$ . In the first step, ferric P450 binds substrate, RH. The P450-substrate complex is then reduced by POR, followed by binding of oxygen. The “second electron” is donated to the oxyferrous P450 by either POR or *cyt*  $b_5$ . The oxygen bond is heterolytically cleaved, resulting in the formation of compound I, the active oxidizing species. An oxygen atom is next inserted into the C–H bond of the substrate. The more hydrophilic product (ROH) dissociates from the active site. The ellipses represent the porphyrin ring while the different colors of the ring indicate spectral differences between the intermediates.  $POR^{\bullet+}$  represents a porphyrin  $\pi$  cation radical

necessary for the effect of *cyt*  $b_5$ . Redox potentials of ferric cytochromes P450 are  $\sim -300$  mV in the absence of substrate and are increased to  $\sim -245$  mV in the presence of substrate, while the potential of *cyt*  $b_5$  is  $\sim +25$  mV (Fig. 2.9) [129, 149–152]. From a thermodynamic perspective, *cyt*  $b_5$  will be unable to reduce ferric P450, but would be able to reduce oxyferrous-bound P450, which is estimated to have a potential of  $\sim +50$  mV [153]. The FMN hydroquinone of POR has an appropriate potential,  $\sim -270$  mV, to reduce the substrate-bound ferric and oxyferrous P450. This enables catalysis to proceed in the absence of *cyt*  $b_5$  [33, 149]. However, the requirement for the reductase to reduce the ferric protein, thereby initiating catalysis, accounts for the observations that *cyt*  $b_5$  acts after the reductase in the catalytic cycle, decreases oxyferrous P450 in hepatic microsomes, and coincides with product formation [141], implying that *cyt*  $b_5$  reduces

oxyferrous P450. Employing the conditional hepatic deletion of both *cyt b<sub>5</sub>* and P450 reductase, Wolf and colleagues were able to demonstrate that *cyt b<sub>5</sub>* reductase and *cyt b<sub>5</sub>* were able to support low levels of P450 activity [140].

When purified proteins became available, it could be demonstrated that *cyt b<sub>5</sub>* could stimulate, inhibit, or have no effect on catalysis by a purified reconstituted P450 and POR [132]. Moreover, these effects were shown to depend on both the particular isozyme of microsomal P450 and the substrate. The sequence of addition of reactants to the assay mixture also influenced the results [154]. To add to the conundrum about the role of *cyt b<sub>5</sub>* in P450 catalysis, it has also been suggested that apo-*cyt b<sub>5</sub>*, lacking the heme, could stimulate catalysis by selected isozymes of P450 [133, 155, 156].

To gain a better understanding of the function of *cyt b<sub>5</sub>* in P450 catalysis, its overall effect on the utilization of NADPH for product formation, rather than side product formation (superoxide and hydrogen peroxide), was investigated by several laboratories [127, 157, 158]. It was concluded that *cyt b<sub>5</sub>* enhanced coupling of NADPH utilization for product formation, i.e., the efficiency of catalysis, by decreasing the formation of the side products, hydrogen peroxide and superoxide.

With P450 2B4, *cyt b<sub>5</sub>* improved the efficiency of NADPH utilization for product formation for both poor and good substrates by approximately ~15% by generating less of the side product superoxide, which rapidly dismutates to hydrogen peroxide. These results suggest an explanation for the substrate dependent effects of *cyt b<sub>5</sub>*. A 15% increase in efficiency of a poor substrate will significantly increase the absolute amount of product formation by a given amount of NADPH. In contrast, a substrate that is already metabolized with a 50% efficiency will not undergo a marked increase in the absolute amount of product formation when the reaction efficiency is simply increased by 15% [157]. *Cyt b<sub>5</sub>* lacking the C-terminus membrane-binding domain has been found by many investigators NOT to enhance P450 activity [127, 159, 160].

### 2.3.4 The Binding Site on P450 for *Cyt b<sub>5</sub>* and P450 Reductase

Having achieved a better understanding of the overall effect of *cyt b<sub>5</sub>* on P450 catalysis, investigators conducted experiments with the goal of elucidating the molecular mechanism by which *cyt b<sub>5</sub>* exerted its influence.

As the heme is buried and not directly accessible on the surface of type I and II P450s, it cannot accept electrons from other protein donors via direct contact between the prosthetic groups. An incoming electron must initially encounter amino acids of the P450 polypeptide [53, 161–163]. The heme is closest to the surface near the axial cysteine, which, by convention, has been designated as the proximal surface of P450. The surface closest to the heme and the cysteine has a positive potential especially in microsomal P450s (P450<sub>cin</sub> 869 Debye; P450<sub>cam</sub> 697 D; P450BM3 640 D; P450 2D6 1197 D; (<http://dipole.weizmann.ac.il/>) P450 17 $\alpha$ -hydroxylase/lyase 1197 D. It is concave with the cysteine at the approximate center and bottom of the concavity. A considerable amount of evidence has accumulated from mutagenesis experiments, ionic strength manipulations, chemical cross-linking studies, crystal structures, and NMR investigations that the anionic, convex surfaces of the redox partners (*cyt b<sub>5</sub>*, P450 reductase, and ferredoxins such as putidaredoxin and adrenodoxin) dock with the basic concave proximal surface of P450 [53, 128, 161, 164–168].

To recap, the interprotein interfaces are complementary with respect to the geometry and electrostatics of their interfaces, which is typical of redox protein interactions [142]. *Cyt b<sub>5</sub>* and POR are promiscuous redox proteins, capable of reducing many different proteins in both physiological and nonphysiological reactions. Thus, it is logical that the specificity of physiological reactions will be dictated by the acceptor protein. A noncognate redox partner might bind and compete with the physiological cognate donor, but if it does mediate catalysis, it usually does so at a markedly slower rate than the cognate reductase

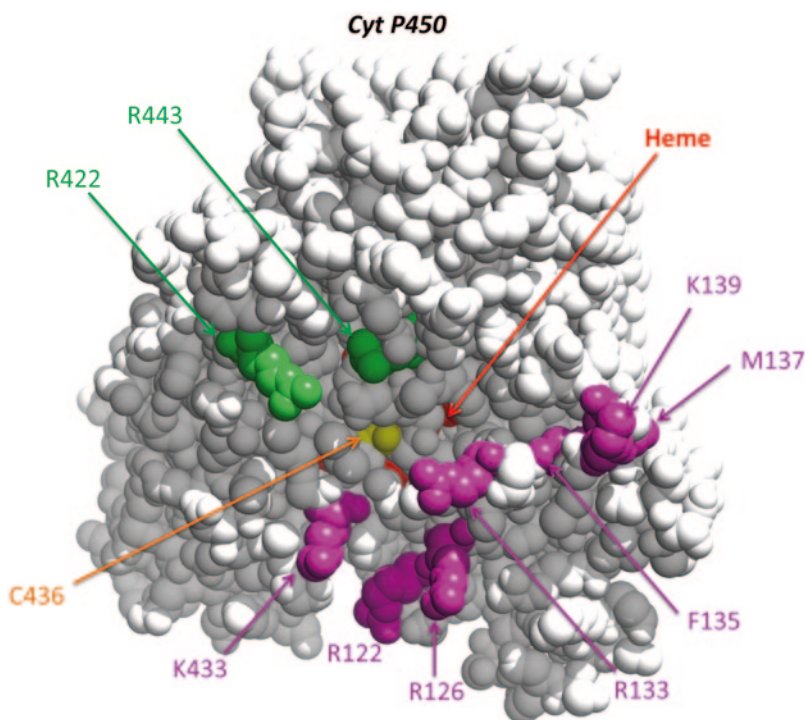


**Fig. 2.10** The binding site for P450 reductase and *cyt b<sub>5</sub>* on the proximal surface of P450 2B4. Residues in *dark pink* are involved either directly or indirectly through a conformational effect in binding both the reductase and

*cyt b<sub>5</sub>*. These residues are in the C helix and the  $\beta$ -bulge. Residues in green are involved only in binding the reductase. They are located in the L helix and between the meander and the  $\beta$ -bulge

[168–170]. Although the microsomal redox partners will bind to the proximal surface of P450, each complex interface will be unique due to the nonidentity of each P450, but nonetheless share many characteristics.

Figure 2.10 illustrates residues on the proximal surface of P450 2B4 (1SUO) that have been demonstrated to participate in redox partner binding, either directly or indirectly, by a conformational change [53]. Residues demonstrated to participate in both *cyt b<sub>5</sub>* and P450 reductase binding are shown in dark pink, while the two residues whose mutation decreases only the affinity for P450 reductase are in green. Both basic and nonpolar residues (F135, M137) are important for the interaction. Another key conclusion from the observation of unique but overlapping binding sites for *cyt b<sub>5</sub>* and reductase is that both cannot be bound to P450 simultaneously. As a result, they will compete for binding to P450. The competition will depend on the relative abun-

dance of each partner and its relative affinity for P450. Even though there is no evidence at this time for a protein corresponding to *cyt b<sub>5</sub>* in either *P. putida*, the source of P450cam or *B. megaterium*, the source of P450BM3, the soluble form of *cyt b<sub>5</sub>* does interact with these P450s on the proximal surface of the respective P450, albeit with significantly (2–3 orders of magnitude) decreased affinity compared to the cognate reductase [170, 171]. As predicted, anionic *cyt b<sub>5</sub>* competes with the acidic putidaredoxin for binding to P450cam [170, 172]. However, *cyt b<sub>5</sub>* does not support rapid catalysis by P450cam. In addition to binding, a specific interaction with a redox partner is required for efficient catalysis [168]. A similar situation exists with P450BM3 which is a dimeric fusion protein between a heme and diflavin P450 reductase domain [171]. Soluble housefly *cyt b<sub>5</sub>* can bind to both the separate P450BM3 heme domain and the intact protein but lacks the ability to enhance the activity of the intact pro-

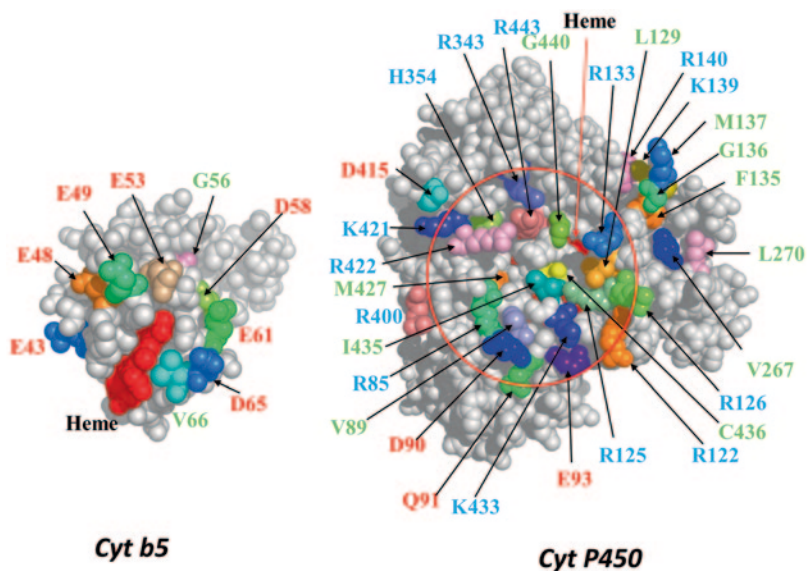


**Fig. 2.11** Composite of interaction sites from different P450s with cyt  $b_5$  and NADPH-cytochrome P450 oxidoreductase (POR). *Left*: Residues from various cyts  $b_5$  that react with different P450s are mapped onto the surface of cyt  $b_5$ .

*Right*: Residues from different P450s that react with POR are mapped onto the proximal surface of P450 2B4 (pdb 1SUO). The basic residue labels are *blue*; acidic residue labels are *red*; neutral residue labels are *green*

tein. Interestingly, intact *E. coli* flavodoxin supports a low level of enzymatic activity of P450 17A1 during expression [173].

In view of the similarity of the proximal surfaces of P450s, residues that have been implicated in the binding of either cyt  $b_5$  or reductase by studies, either in humans or in vitro, have been mapped onto the proximal surface of P450 2B4 (pdb code 1SUO (Fig. 2.11) [174]. These residues are located in the B, C, J, K, H, and L helices, the  $\beta$ -bulge, and the residues between the meander and  $\beta$ -bulge. Data from the following P450s have been included in Fig. 2.11: CYP101, CYP102, CYP1A1, CYP1A2, CYP2A5, CYP2B1, CYP2B4, CYP2C8, CYP2C9, CYP2E1, CYP3A4, CYP6AB3, CYP17A1, CYP19. [65, 87, 134, 164, 166, 167, 169, 172, 175–185]. Figure 2.11 demonstrates that the P450s, for which there is structural information about the docking surface, all interact with their redox partners on the proximal surface as proposed [161]. Although basic residues predominate, hydrophobic residues and hydrogen bonds

also contribute to the docking interface between the partners [87].

Selected proteins (CYP101, CYP1A2, CYP3A4, CYP6AB3, CYP19) appear to dock with the reductase in the B–B' helix (residues R85, V89, D90, Q91) which is close to the substrate binding site and the I helix. Reductase binding at this site might induce conformational changes in the active site. Many of the P450 residues in the C helix,  $\beta$ -bulge, and N-terminus of the L helix have been demonstrated to be essential to the interprotein complex for both reductase and cyt  $b_5$ . In view of the proximity of the C helix and  $\beta$ -bulge to the heme, many of the residues in these secondary structures contact the heme. It is not unexpected that their residues would be important for redox partner interactions. Structural evidence (from the > 100 P450 structures in the pdb) is also accumulating that redox partner binding transmits conformational and dynamic changes to the active site and that conformational changes from the active site can be transmitted to the proximal surface. Substrate binding to

P450s typically decreases the flexibility of residues involved in substrate binding and modifies the architecture of the active site. Substrate and inhibitor binding may also modify the conformation of the redox partner-binding site. P450s are extraordinarily flexible molecules, well suited to perform their numerous functions [168, 186, 187].

Examination of Fig. 2.11 demonstrates that there is a ring of basic residues (R443, R133, R126, R125, R122, K433, R85, R422, K421, H354, R343) around the rim of the depression on the proximal surface, which is also present with some variation on the proximal surface of other P450s. The long, flexible basic residues which are components of this rim are in an excellent position to “electrostatically steer” and dock with the negatively charged surface of the redox partner to form an encounter complex (Fig. 2.6). In view of current knowledge, it appears that each P450 employs slightly different residues to react with its promiscuous redox partners. In humans, there is a single reductase that provides electrons to approximately fifty microsomal P450s and heme oxygenases, while cyt  $b_5$  also reacts with several very different redox partners (desaturases and enzymes involved in the synthesis and biodegradation of lipids [127]). It is, therefore, necessary for the P450 to provide the specificity of the reaction. For example, three residues (Arg347, Arg358, Arg449) on the proximal surface of P450 17 $\alpha$ -hydroxylase form a positively charged patch critical for cyt  $b_5$  binding [160, 165]. Mutation of these residues preferentially diminished the binding and lyase activity of cyt  $b_5$  compared to the binding and 17 $\alpha$ -hydroxylase activity of the reductase, consistent with the notion that the P450 controls the specificity of the interaction with the redox partners [188].

### 2.3.5 Binding Site on Cyt $b_5$ for P450

The sequence of the soluble, negatively charged, heme-binding domain of microsomal cyts  $b_5$  is highly conserved in eukaryotes with about 80% identity and very conservative substitutions. The two most conserved motifs are the HPGG,

which includes one of the axial histidines, and the GXDATD/E. In mammals, the glutamate and aspartic residues are completely conserved, while Asp58 is the most highly conserved acidic residue among all the different cyts  $b_5$  [189]. The plant heme-binding cyt  $b_5$  domains are ~50% similar [166, 190]. Mutagenesis, cross-linking, and modeling studies indicate that anionic residues surrounding the solvent exposed cyt  $b_5$  heme are important for binding to P450, as is a heme propionate. Most of the residues implicated in participating in binding to P450s are on or near the loops that host the two axial histidines (H44, H68), i.e., the “40s” and “60s” loops between  $\alpha$ -helices 2 and 3 and  $\alpha$ -helices 4 and 5, respectively [128, 134, 165, 166, 191–194]. An exception is the highly conserved Asp58 located ~14 Å away from the 60s loop [190]. Since it is located in a loop between  $\beta$ -strand 5 and the start of helix  $\alpha$ -4, it may have a structural role and, as a result, may be altering the 60s loop conformation. A heme propionate has also been implicated in binding P450 (Figs. 2.12 and 2.13) [127, 128, 134]. Figure 2.11 illustrates the anionic surface of cyt  $b_5$  with the location and identification of amino acids whose mutation has resulted in decreased interaction with a number of different P450s, respectively [127, 128, 134, 165, 166, 191–194]. Note the paucity of cyt  $b_5$  residues deemed important for binding to P450s and that it was sometimes necessary to construct a double mutant to observe a significant decrease in function. This observation is consistent with the conclusion of Dutton and coworkers, namely that in nature interprotein electron transfer has generally been engineered to be robust and resistant to mutational changes and minor perturbations by positioning the electron donor and acceptor within 14 Å [142]. In one study, 13 residues surrounding the heme were mutated to alanine [128]. Eleven of the residues had no or only a very modest effect on the interaction with P450 2B4. Of the eleven amino acids shown not to contribute significant energy to the binding of P450 2B4, four of them (G49, V50, E53, Q54) were in contact with P450 2B4 in models of a major and minor complex between cyt  $b_5$  and P450 2B4 (Figs. 2.12 and 2.13). Interestingly, one of the two residues observed

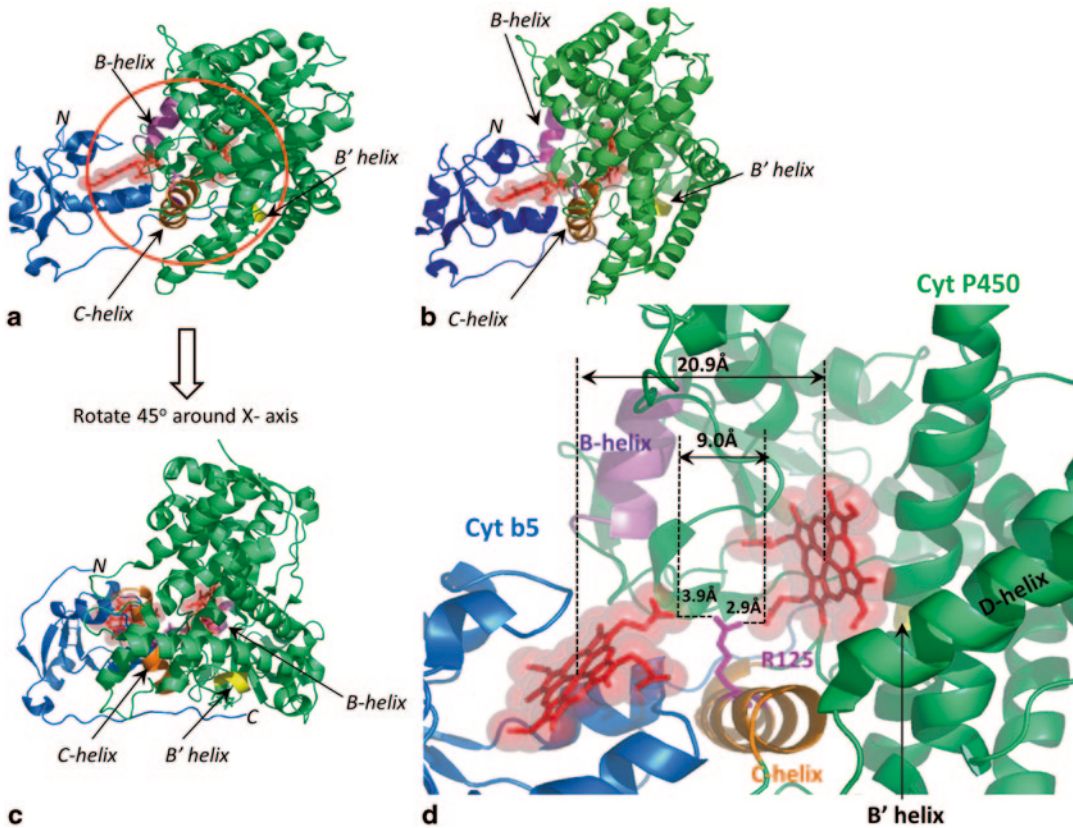


**Fig. 2.12** Overview of the structure of a major and minor cyt *b*<sub>5</sub>-P450 2B4 complex. Mutagenesis and NMR constraints were employed to determine the complex structures. P450 2B4 is in *green*; cyt *b*<sub>5</sub> is in *blue*; heme is in *red*; P450 Arg125 is in *magenta*. **a** The most abundant complex as determined by nuclear magnetic resonance (NMR). **b** The less abundant complex [128]. Note how

little movement is necessary for both the 40s and 60s loops to come in contact with P450. **c** Rotation of the major complex to show the location of the terminus of the flexible linker. **d** Electron transfer predicted by HARLEM to occur between the cyt *b*<sub>5</sub> and P450 heme D propionates via P450 Arg125 [128]

to contribute most to the binding energy of the complex was hydrophobic Val66, the other was Asp65 [128].

### 2.3.6 Model of the P450 2B4 and Cyt *b*<sub>5</sub> Complex

On the basis of mutagenesis data from seven P450 2B4 mutants and 13 cyt *b*<sub>5</sub> mutants, a double mutant cycle analysis, and NMR-generated constraints, a model of the P450 2B4-cyt *b*<sub>5</sub> complex has been constructed using the docking algorithm HADDOCK [128]. HADDOCK first docks the two proteins as rigid bodies to minimize intermolecular energy. Next, it allows

residues at the interface to move to optimize side chain and backbone orientations. Finally, the structures are refined in explicit solvent layers. Major and minor complexes were observed, indicating the dynamic nature of the complexes (Figs. 2.12 and 2.13). In the major complex, residues in the “60s loop,” which flanks axial His68, are in contact with P450, whereas in the minor complex, the cyt *b*<sub>5</sub> is slightly tilted so that residues in both the “40s” and “60s” loops are in contact with P450 2B4. Altogether seventeen cyt *b*<sub>5</sub> residues were in contact with P450 2B4. Models of the cyt *b*<sub>5</sub>-P450 3A4 and cyt *b*<sub>5</sub>-P450 2E1 complexes, together with mutagenesis data, also indicate that the “60s loop” is likely the primary area of contact with these P450s [134, 166].

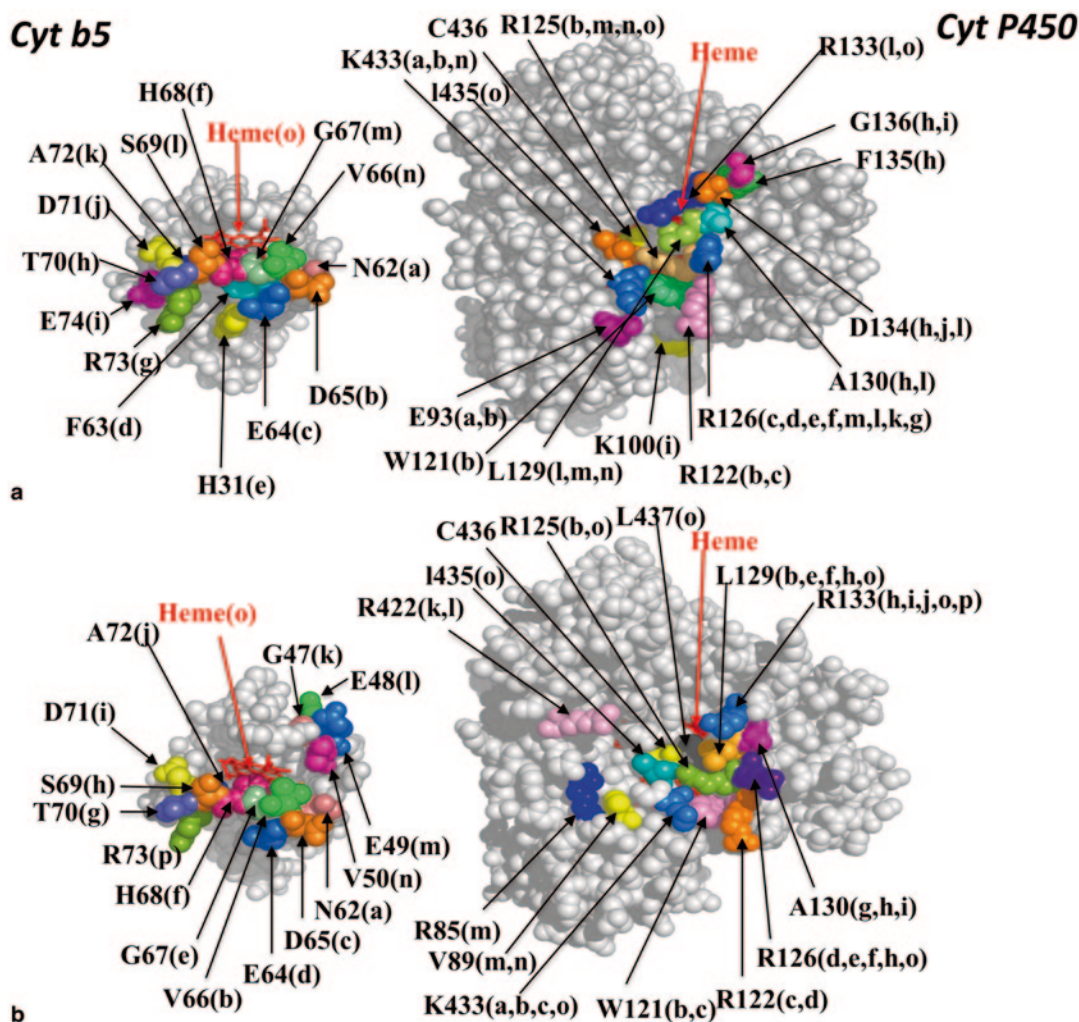


**Fig. 2.13** Interface of the major and minor *cyt b*<sub>5</sub>-P450 2B4 complexes. **a** The residues in contact on the interface of the most abundant, major complex. Residues on P450 that are in contact with residues on *cyt b*<sub>5</sub> are denoted with matching letters in parenthesis. For example, Arg133 (l, o) on P450 (dark blue) is in contact with Ser69 (l) and heme (o) on *cyt b*<sub>5</sub>. *Cyt b*<sub>5</sub> is on the left and P450 on the right (pdb codes 2M33 and 1SUO respectively). Most of the

*cyt b*<sub>5</sub> residues in contact with P450 are located in or near the 60s loop. Residues on *cyt b*<sub>5</sub> that are in contact with residues on P450 are denoted with matching letters in parentheses. **b** Interface of the less abundant *cyt b*<sub>5</sub>-P450 complex. Note that many of the residues are the same. The most noticeable difference is that both the 40s and 60s loop of *cyt b*<sub>5</sub> are in contact with P450 [128]

Mutagenesis experiments suggest that the “40s loop” is involved in binding to P450 17A1, while P450 2C19 interacts with the residues in the “60s loop” [192].

The most notable feature of the complex is the salt bridge formed by the highly conserved Arg125 of P450 between the heme D propionates of both *cyt b*<sub>5</sub> and P450 2B4. Arg125 of P450

2B4 is homologous to P450<sub>cam</sub> Arg112, which has been shown to be essential for interprotein electron transfer [182]. HARLEM, an electron transfer pathways prediction program, proposed that electron transfer may occur between the heme propionates [128]. The heme edges are 9 Å apart, while the heme irons are separated by 20.9 Å, well within the generally accepted

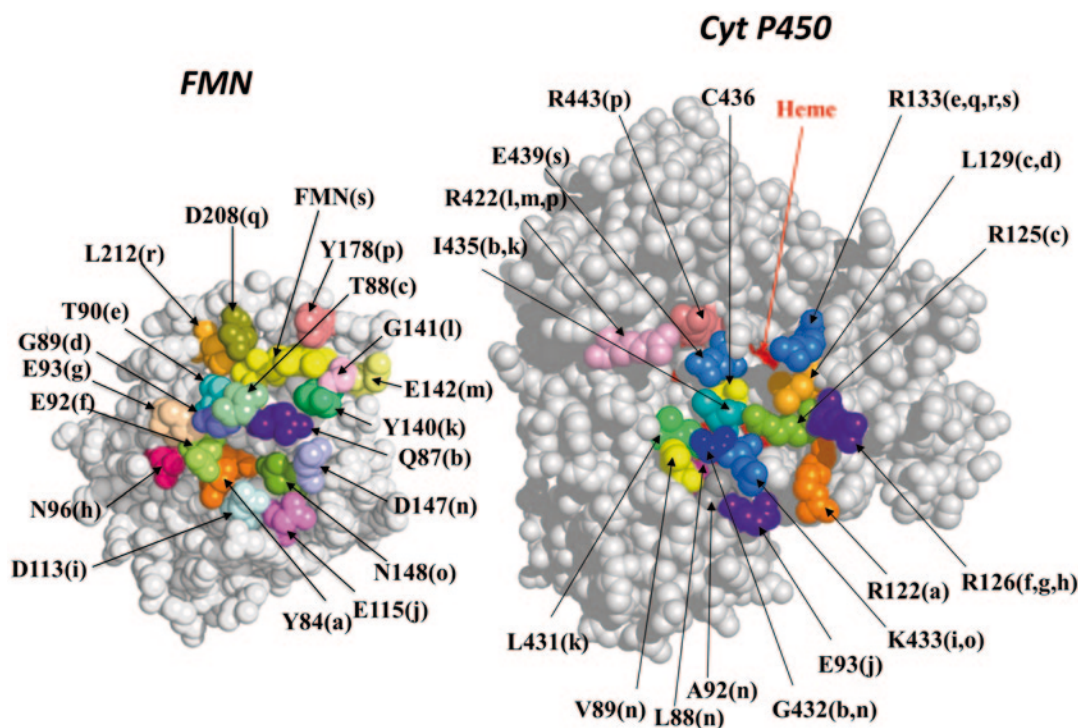


**Fig. 2.14** Interface of the NADPH-cytochrome P450 oxidoreductase (POR)—flavin mononucleotide (FMN) domain—P450 2B4 complex. The model was generated as previously described, using mutagenesis constraints

[52]. The coordinates of the FMN domain were from pdb code 3ES9 and from pdb code 1SUO for P450 2B4. Residues on the FMN domain that are in contact with P450 are denoted with matching letters in parenthesis

electron tunneling distance of 14 Å [142]. The surface area of the complex interface is ~1150 Å<sup>2</sup>. It is formed by salt bridges, hydrogen bonds, and hydrophobic residues, as proposed for electron transfer proteins [87]. Results of a double mutant cycle analysis revealed that P450 2B4 Lys433, located three residues upstream of axial Cys436 in the β-bulge, was in contact with the acidic amino acid Asp65 and the hydrophobic Val66 of *cyt b<sub>5</sub>*. Arg122 in the P450 C helix interacts with Asp65 [128]. Lysines, in CYP2E1, CYP1A2, and CYP2C9 that are homologous to Lys433 have been implicated in binding its redox partners. Due to its proximity to the heme, Lys433 and homologous lysines are well situated to transmit structural information from the redox partner to P450 and perhaps electrons.

For comparison, Fig. 2.14 shows the residues in contact in the model of the complex between P450 2B4 and the FMN domain of P450 reductase. Figure 2.5 provides an overview of the

complex [53]. Interprotein contacts include salt bridges, hydrogen bonds, and van der Waals interactions. The area of the interface of the FMN domain-P450 complex is 870 Å<sup>2</sup>, slightly smaller than the *cyt b<sub>5</sub>*-P450 interface. It can be seen that P450 residues implicated in binding P450 reductase also participate in binding *cyt b<sub>5</sub>*. While the different P450s all appear to utilize their proximal surface for docking, each proximal surface is unique. The interprotein complexes will be similar, but not identical, and will be formed based on the general principles of interprotein complex formation. Homologous residues may make quantitatively different contributions to the binding energy of their respective complexes. Utilization of overlapping but nonidentical sites for P450 reductase and *cyt b<sub>5</sub>* binding predicts the redox partners will compete for binding to P450 and their binding will be mutually exclusive. Experiments with P450 2B4, P450 17A1, and P450 3A4 demonstrate that *cyt b<sub>5</sub>* and P450 reductase



do, indeed, compete for docking with P450 [128, 134, 165]. In a particular situation, the relative affinity of the redox partners for P450 and the relative concentration of cyt  $b_5$  and the reductase will determine which partner actually binds to the P450. How the binding of microsomal P450s to their partners is orchestrated *in vivo* is unknown. Since there are alleged to be ~5–20 molecules of P450 for every reductase molecule in microsomes, the *in vivo* regulation of the interprotein reaction is presumed to be highly regulated by a currently unknown mechanism. [22, 23, 195].

### 2.3.7 Mechanism of Action of Cyt $b_5$ with P450

The possible mechanisms of action of cyt  $b_5$  with P450 have been reviewed [127]. The proposed mechanisms of action will be summarized and then discussed in light of recent experiments that have begun to provide some clarity (see Fig. 2.9 for the P450 reaction cycle). (1) One possibility is that cyt  $b_5$  provides the second electron to oxyferrous P450 faster than POR. (2) The second possibility is that cyt  $b_5$  enhances the utilization of NADPH for product formation, possibly because it provides the second electron faster than P450 reductase. (3) The third possibility is that P450, POR, and cyt  $b_5$  form a ternary complex. Reductase delivers two electrons to the diheme complex via P450. Reductase then dissociates from the ferrous diheme complex. After oxygen binds to P450, the ferrous cyt  $b_5$  immediately reduces oxyferrous P450. It was proposed that reduction of oxyferrous P450 by bound cyt  $b_5$  would occur faster than reductase dissociation to retrieve a second electron. (4) The fourth possibility is that cyt  $b_5$  acts as an effector in the reaction with P450.

1. When the rates of reduction of an oxyferrous microsomal P450 by cyt  $b_5$  and P450 reductase were directly measured and compared, it was observed that cyt  $b_5$  and reductase both reduced oxyferrous P450 2B4 at the same rate [149]. Unexpectedly, the P450 reacted differently following reduction, depending on whether it had accepted an electron from cyt

$b_5$  or POR. Presumably this occurs because each redox partner elicited a different conformational change in the active site on the distal side of the heme. In the presence of cyt  $b_5$ , product was formed rapidly with the substrate benzphetamine and with ~52% coupling, whereas product formation was significantly slower (~10–100-fold) and less coupled (~32%) with the reductase. Coupling refers to utilization of electron equivalents for product formation. How much slower depends on the substrate [196]. How generalizable a phenomenon and observation this is awaits the results with different P450 isozymes.

2. Numerous investigators have indeed shown that cyt  $b_5$  may enhance the coupling of NADPH utilization for product formation at the expense of side product (hydrogen peroxide and superoxide) formation [157, 158, 197]. While this is a reproducible observation, it is not a molecular explanation for the actions of cyt  $b_5$ . Increased efficiency of NADPH utilization could be explained by the more rapid rate of product formation, which allows less time for production of the side products hydrogen peroxide and superoxide.
3. While it was established as early as the 1980s that ferrous P450 could reduce ferric cyt  $b_5$ , the role of such a reaction in altering the activity in a reconstituted system is uncertain [158, 198, 199]. Moreover, the alleged formation of a ternary complex between P450, cyt  $b_5$ , and P450 reductase has been challenged [57, 200]. A functional ternary complex is also incompatible with the large amount of mutagenesis data that reveals cyt  $b_5$  and the reductase have overlapping binding sites on the proximal surface of P450s and with observations from several laboratories on purified reconstituted systems that the redox partners compete with one another for a binding site on P450 [134, 139, 165].
4. There is a significant amount of evidence from a number of laboratories that cyt  $b_5$  can act as an effector for some P450s. P450 2D6 and P450 1A1 are known exceptions [201]. One of the earliest and most convincing examples is the partial conversion of the hexacoordinate

low-spin to the pentacoordinate high-spin heme iron, which occurs when cyt  $b_5$  binds to a P450 (2B4, 3A4, 17A1, 4A7). Displacement of the sixth axial ligand, water, from the heme of P450 by cyt  $b_5$  in many instances is greater when substrate is present in the active site. One of the simplest explanations for the displacement of the water from the P450 heme iron is a conformational change induced by the binding of cyt  $b_5$  that is subsequently transmitted to the active site, resulting in the displacement of water from the iron. In view of the tremendous flexibility of P450s exhibited by the P450 atomic resolution crystal structures, there are several plausible pathways through which conformational changes could be propagated from the proximal surface to the distal substrate-binding pocket. One is that docking with residues on the C helix can transmit changes via the substrate-binding B-B' loop and helices to the I helix near the conserved active site threonine and acidic residue.

Of the four previously proposed mechanisms of action of cyt  $b_5$ , it appears that there is insufficient evidence for ternary complex formation and a more rapid reduction of oxyferrous P450 by cyt  $b_5$  compared to POR. Both reduce P450 at the same rate. It is proposed that cyt  $b_5$  simultaneously has two effects on the P450 isozymes it stimulates. Its interaction with P450 results in both electron donation to the oxyferrous protein and a substrate- and isozyme-dependent conformational change in the active site that allows catalysis to occur more rapidly. One possibility is that the active site conformational change induced by cyt  $b_5$  leads to the more rapid formation of the active oxygenating species, compound I, compared to the reductase [158, 196]. The more rapid turnover in the presence of cyt  $b_5$  results in less time for side product formation, which in turn increases the coupling of NADPH consumption to product formation.

### 2.3.8 Apo Cytochrome $b_5$

Currently, there is no consensus about whether apo cyt  $b_5$  (cyt  $b_5$  devoid of heme) is able to act

only allosterically to stimulate catalysis by P450 or whether apo cyt  $b_5$  must first bind heme to form holo cyt  $b_5$ , which is both capable of electron transfer and an allosteric effect. One of the difficulties in analyzing the literature about apo cyt  $b_5$  is that dissimilar conditions have been employed to investigate not only different isozymes but also identical proteins, precluding a satisfying conclusion about the effects of apo cyt  $b_5$  on P450 catalysis. NMR studies have shown that the structure of apo cyt  $b_5$  and cyt  $b_5$  are similar, with only minimal differences in their secondary structure [202]. As a result, they are expected to have a similar interaction with P450s. Models of a complex between P450 3A4 and apo cyt  $b_5$  and holo cyt  $b_5$  have been constructed. They indicate that both complexes form very similar docking sites on the proximal surface of P450 3A4 in a location that overlaps with the POR binding site [134].

Apo cyt  $b_5$  has been found to stimulate some P450s (P450 3A4, the 17,20-lyase reaction of P450 17A1, and P450s 2A6, 2C8, 2C9, 2C19, 3A5, 4A4, 4A7 and 6A1) [133, 134, 155, 156, 158, 197, 201], but not others (P450 2B4, 2E1, and 2D6) [132, 133, 137, 203]. Apo cyt  $b_5$  can only stimulate a P450 activity if the holo cyt  $b_5$  can enhance the activity. Apo cyt  $b_5$  has also been reported to induce a spin-state change in some P450s, which indicates that apo cyt  $b_5$  binds to P450. This is not surprising in view of their similar structures [134].

Recently, the allosteric stimulatory effector role of apo cyt  $b_5$  was challenged [204, 205]. It was proposed that the stimulatory effect of apo cyt  $b_5$  was due to the transfer of heme from P450 3A4 and P450 17A1 to apo cyt  $b_5$ , thereby creating holo cyt  $b_5$ , which is known to possess stimulatory properties. A more compelling argument about the lack of the stimulatory ability of apo cyt  $b_5$  was their demonstration that neither a redox inactive Zn-substituted protoporphyrin IX derivative of cyt  $b_5$  nor an axial His67Ala mutant that is unable to bind heme was able to stimulate the activity of either P450 3A4 or P450 17A1. Moreover, the addition of a heme scavenger, apo myoglobin, to the reaction mixture eliminated the stimulatory effects of the apo cyt  $b_5$ .

These studies prompted a reexamination of the stimulatory effects of apo cyt  $b_5$  in a reconstituted system with P450 3A4 and 17A1 [133]. The reexamination concluded that far less heme transfer occurred than could be accounted for by the stimulatory effects of apo cyt  $b_5$ . Furthermore, apo myoglobin did not inhibit the stimulatory effects of apo cyt  $b_5$ . The reexamination did not include investigation of the effects of redox inactive cyt  $b_5$  which had been reconstituted with a Zn-substituted protoporphyrin IX. Nor did it investigate whether cyt  $b_5$  mutants that were unable to bind heme were still stimulatory.

Several laboratories have reported that cyt  $b_5$  reconstituted with Mn protoporphyrin IX, which is redox inactive in the reconstituted system, was unable to stimulate the activity of P450 [132, 139, 200, 206, 207]. In fact, as the concentration of Mn cyt  $b_5$  was increased relative to a constant amount of P450 and P450 reductase, NADPH consumption and activity decreased and the rate of reduction of ferric P450 was diminished. These effects of Mn cyt  $b_5$  are consistent with the ability of Mn cyt  $b_5$  to decrease the rate of reduction of ferric P450 by competing with P450 reductase for binding to P450 [139]. In addition, it has been reported that siblings with a homozygous axial histidine variant of cyt  $b_5$ , His44Leu, exhibited a phenotype with abnormal genitalia and low androgens, indicative of an apparently isolated deficiency of the cyt  $b_5$  requiring 17,20-lyase activity of P450 17A1. An elevated methemoglobin ( $\text{Fe}^{+3}$  Hb) was also noted. This human phenotype is supportive of a nonfunctional apo cyt  $b_5$  in vivo [208]. Drug metabolism was not investigated in these individuals.

In conclusion, in spite of the different isozymes and experimental conditions involved, apo cyt  $b_5$  does appear to affect the activity of selected P450s. Its mechanism of action continues to be vigorously debated. Nevertheless, the weight of the evidence is pointing to the likelihood that only P450s that are able to transfer their heme to apo cyt  $b_5$  to form holo cyt  $b_5$  and also have activities that are increased by holo cyt  $b_5$  are stimulated. For example, P450 3A4 and 17A1 have been observed to transfer heme to apo cyt  $b_5$  under experimental conditions, whereas

P450 2B4 does not significantly transfer heme to apo cyt  $b_5$ . Due to the similarity of apo- and holo cyt  $b_5$  structures, apo cyt  $b_5$  may also compete with reductase for a docking site on P450, which, depending on the molar ratios of the redox partners to P450 and their relative affinities for P450, could decrease the activity of the isozyme even in the absence of holo cyt  $b_5$  formation.

### 2.3.9 Summary of Mechanism of Action of Cyt $b_5$ on P450

Although our understanding of how cyt  $b_5$  can increase, decrease, or have no effect on catalysis by P450, and why its actions are dependent on the isozyme and substrate, is still incomplete, significant progress has been made in the past four decades in elucidating its mechanism of action. The fact that both cyt  $b_5$  and reductase reduce oxyferrous P450 at the same rate indicates that the mechanism of action of cyt  $b_5$  occurs after reduction of oxyferrous P450 in the reaction cycle. Its stimulatory effects are consistent with an ability to generate the active oxidizing oxyferryl species, compound I, more rapidly than P450 reductase. It is likely that this occurs by inducing a conformational change in the proton delivery network in the P450 active site. More rapid formation of compound I would allow less time for side product formation and result in increased efficiency of catalysis.

Evidence is also accumulating that is supportive of the notion that cyt  $b_5$  and reductase compete for a binding site on the basic proximal surface of P450s. The ability of a redox partner to bind a P450 will depend on the relative concentrations and relative affinities of the redox partners for the specific P450 isozyme. At higher molar ratios compared to a constant P450:POR 1:1 ratio, cyt  $b_5$  will abort the reaction cycle by preventing P450 reductase from reducing ferric P450, while at lower molar ratios cyt  $b_5$  is stimulatory [196]. No effect is observed when the opposite effects cancel. The actions of cyt  $b_5$  on different isozymes of P450 is inferred to depend on its ability to induce the conformational changes in the active site necessary for more rapid catalysis and on

its affinity for the particular P450 in comparison to the POR.

A final dilemma is: why does the effect of cyt  $b_5$  vary with the substrate even when it is being metabolized by the same P450? This is the least understood, most enigmatic of the effects of cyt  $b_5$ . It has been observed that under similar conditions, the same P450 utilizes qualitatively the same amount of NADPH regardless of the substrate, while cyt  $b_5$  increases the efficiency of catalysis by roughly 15% regardless of the substrate [157]. These results lead to the speculation that a poor substrate whose metabolism is 2% coupled will have the absolute amount of its metabolism increased by ~ seven times. In contrast, a good substrate whose metabolism is approximately 50% coupled will have the absolute value of its metabolism enhanced by merely 30%, which may be within experimental error [157]. How generalizable this speculation is awaits detailed studies of other P450s and substrates. Both reactions should be subject to inhibition by high concentrations of cyt  $b_5$ . If cyt  $b_5$  really does increase the efficiency of catalysis by approximately the same amount irrespective of the substrate, it implies that its putative allosteric effect is probably not always dependent on the substrate. The highly flexible nature of P450s has been noted and likely contributes to the variety of results.

**Acknowledgments** The authors wish to thank all investigators who have studied the interaction of P450 with its redox partners. We regret it has not been possible to cite all publications. We wish to acknowledge Sangchoul Im, Yuting Yang, and Chuanwu Xia for the preparation of the figures. The work was supported by a Veterans Affairs Merit Review grant and NIH grants GM094209 to LW and GM097031 to JJK.

## References

- Guengerich FP (2008) Cytochrome P450 and chemical toxicology. *Chem Res Toxicol* 21:70–83
- Roman LJ, Masters BS (2010) The cytochromes P450 and nitric oxide synthases. In: Devlin TM (ed) *Textbook of biochemistry with clinical correlations*, 7th edn. Wiley, New York, pp 425–456
- Hannemann F, Bichet A, Ewen KM, Bernhardt R (2007) Cytochrome P450 systems—biological variations of electron transport chains. *Biochim Biophys Acta* 1770:330–344
- Stuehr DJ, Tejero J, Haque MM (2009) Structural and mechanistic aspects of flavoproteins: electron transfer through the nitric oxide synthase flavoprotein domain. *FEBS J* 276:3959–3974
- Daff S (2010) NO synthase: structures and mechanisms. *Nitric Oxide Biol Chem* 23:1–11
- Feng C (2012) Mechanism of nitric oxide synthase regulation: electron transfer and interdomain interactions. *Coord Chem Rev* 256:393–411
- Iyanagi T, Xia C, Kim JJ (2012) NADPH-cytochrome P450 oxidoreductase: prototypic member of the diflavin reductase family. *Arch Biochem Biophys* 528:72–89
- Ruettinger RT, Wen LP, Fulco AJ (1989) Coding nucleotide, 5' regulatory, and deduced amino acid sequences of P-450BM-3, a single peptide cytochrome P-450:NADPH-P-450 reductase from *Bacillus megaterium*. *J Biol Chem* 264:10987–10995
- Ostrowski J, Barber MJ, Rueger DC, Miller BE, Siegel LM, Kredich NM (1989) Characterization of the flavoprotein moieties of NADPH-sulfite reductase from *Salmonella typhimurium* and *Escherichia coli*. Physicochemical and catalytic properties, amino acid sequence deduced from DNA sequence of *cysJ*, and comparison with NADPH-cytochrome P-450 reductase. *J Biol Chem* 264:15796–15808
- Leclerc D, Wilson A, Dumas R, Gafuik C, Song D, Watkins D, Heng HH, Rommens JM, Scherer SW, Rosenblatt DS, Gravel RA (1998) Cloning and mapping of a cDNA for methionine synthase reductase, a flavoprotein defective in patients with homocystinuria. *Proc Natl Acad Sci U S A* 95:3059–3064
- Olteanu H, Benerjee R (2001) Human methionine synthase reductase, a soluble P450 reductase-like dual flavoprotein, is sufficient for NADPH-dependent methionine synthase activation. *J Biol Chem* 276:35558–35563
- Wolthers KR, Lou X, Toogood HS, Leys D, Scrutton NS (2007) Mechanism of coenzyme binding to human methionine synthase reductase revealed through the crystal structure of the FNR-like module and isothermal titration calorimetry. *Biochemistry* 46:11833–11844
- Paine MJ, Garner AP, Powell D, Sibbald J, Sales M, Pratt N, Smith T, Tew DG, Wolf CR (2000) Cloning and characterization of a novel human dual flavin reductase. *J Biol Chem* 275:1471–1478
- Inui H, Yamaji R, Saidoh H, Miyatake K, Nakano Y, Kitaoka S (1991) Pyruvate:NADP<sup>+</sup> oxidoreductase from *Euglena gracilis*: limited proteolysis of the enzyme with trypsin. *Arch Biochem Biophys* 286:270–276
- Nakazawa M, Inui H, Yamaji R, Yamamoto T, Takenaka S, Ueda M, Nakano Y, Miyatake K (2000) The origin of pyruvate: NADP<sup>+</sup> oxidoreductase in mitochondria of *Euglena gracilis*. *FEBS Lett* 479:155–156
- Netz DJ, Stumpfig M, Dore C, Muhlenhoff U, Pierik AJ, Lill R (2010) Tah18 transfers electrons to Dre2 in cytosolic iron-sulfur protein biogenesis. *Nat Chem Biol* 6:758–765
- Schacter BA, Nelson EB, Marver HS, Masters BS (1972) Immunochemical evidence for an association

- of heme oxygenase with the microsomal electron transport system. *J Biol Chem* 247:3601–3607
18. Guengerich FP (2005) Reduction of cytochrome  $b_5$  by NADPH-cytochrome P450 reductase. *Arch Biochem Biophys* 440:204–211
  19. Ono T, Takahashi K, Odani S, Konno H, Imai Y (1980) Purification of squalene epoxidase from rat liver microsomes. *Biochem Biophys Res Comm* 96:522–528
  20. Pearson JT, Siu S, Meininger DP, Wienkers LC, Rock DA (2010) *In vitro* modulation of cytochrome P450 reductase supported indoleamine 2,3-dioxygenase activity by allosteric effectors cytochrome  $b_5$  and methylene blue. *Biochemistry* 49:2647–2656
  21. Petersen JA, Ebel RE, O’Keeffe DH, Matsubara T, Estabrook RW (1976) Temperature dependence of cytochrome P-450 reduction. A model for NADPH-cytochrome P-450 reductase:cytochrome P-450 interaction. *J Biol Chem* 251:4010–4016
  22. Shephard EA, Phillips IR, Bayney RM, Pike SF, Rabin BR (1983) Quantification of NADPH: cytochrome P-450 reductase in liver microsomes by a specific radioimmunoassay technique. *Biochem J* 211:333–340
  23. Backes WL, Kelley RW (2003) Organization of multiple cytochrome P450s with NADPH-cytochrome P450 reductase in membranes. *Pharmacol Ther* 98:221–233
  24. Johnson EF, Stout CD (2005) Structural diversity of human xenobiotic-metabolizing cytochrome P450 monooxygenases. *Biochem Biophys Res Comm* 338:331–336
  25. Johnson EF, Stout CD (2013) Structural diversity of eukaryotic membrane cytochrome P450s. *J Biol Chem* 288:17082–17090
  26. Iyanagi T, Mason HS (1973) Some properties of hepatic reduced nicotinamide adenine dinucleotide phosphate-cytochrome c reductase. *Biochemistry* 12:2297–2308
  27. Iyanagi T, Makino R, Anan FK (1981) Studies on the microsomal mixed-function oxidase system: mechanism of action of hepatic NADPH-cytochrome P-450 reductase. *Biochemistry* 20:1722–1730
  28. Iyanagi T, Makino N, Mason HS (1974) Redox properties of the reduced nicotinamide adenine dinucleotide phosphate-cytochrome P-450 and reduced nicotinamide adenine dinucleotide-cytochrome  $b_5$  reductases. *Biochemistry* 13:1701–1710
  29. Das A, Sligar SG (2009) Modulation of the cytochrome P450 reductase redox potential by the phospholipid bilayer. *Biochemistry* 48:12104–12112
  30. Brenner S, Hay S, Munro AW, Scrutton NS (2008) Inter-flavin electron transfer in cytochrome P450 reductase—effects of solvent and pH identify hidden complexity in mechanism. *FEBS J* 275:4540–4557
  31. Munro AW, Noble MA, Robledo L, Daff SN, Chapman SK (2001) Determination of the redox properties of human NADPH-cytochrome P450 reductase. *Biochemistry* 40:1956–1963
  32. Vermilion JL, Coon MJ (1978) Identification of the high and low potential flavins of liver microsomal NADPH-cytochrome P-450 reductase. *J Biol Chem* 253(24):8812–8819
  33. Oprian DD, Coon MJ (1982) Oxidation-reduction states of FMN and FAD in NADPH-cytochrome P-450 reductase during reduction by NADPH. *J Biol Chem* 257:8935–8944
  34. Oprian DD, Gorsky LD, Coon MJ (1983) Properties of the oxygenated form of liver microsomal cytochrome P-450. *J Biol Chem* 258:8684–8691
  35. Porter TD, Kasper CB (1986) NADPH-cytochrome P-450 oxidoreductase: flavin mononucleotide and flavin adenine dinucleotide domains evolved from different flavoproteins. *Biochemistry* 25:682–1687
  36. Wang M, Roberts DL, Paschke R, Shea TM, Masters BS, Kim JJ (1997) Three-dimensional structure of NADPH-cytochrome P450 reductase: prototype for FMN- and FAD-containing enzymes. *Proc Natl Acad Sci U S A* 94:8411–8416
  37. Karplus PA, Daniels MJ, Herriott JR (1991) Atomic structure of ferredoxin-NADP+ reductase: prototype for a structurally novel flavoenzyme family. *Science* 251:60–66
  38. Smith GC, Tew DG, Wolf CR (1994) Dissection of NADPH-cytochrome P450 oxidoreductase into distinct functional domains. *Proc Natl Acad Sci U S A* 91:8710–8714
  39. Hodgson AV, Strobel HW (1996) Characterization of the FAD binding domain of cytochrome P450 reductase. *Arch Biochem Biophys* 325:99–106
  40. Garcin ED, Bruns CM, Lloyd SJ, Hosfield DJ, Tiso M, Gachhui R, Stuehr DJ, Tainer JA, Getzoff ED (2004) Structural basis for isozyme-specific regulation of electron transfer in nitric-oxide synthase. *J Biol Chem* 279:37918–37927
  41. Black SD, Coon MJ (1982) Structural features of liver microsomal NADPH-cytochrome P-450 reductase. Hydrophobic domain, hydrophilic domain, and connecting region. *J Biol Chem* 257:5929–5938
  42. Porter TD, Kasper CB (1985) Coding nucleotide sequence of rat NADPH-cytochrome P-450 oxidoreductase cDNA and identification of flavin-binding domains. *Proc Natl Acad Sci U S A* 82:973–977
  43. Taniguchi H, Imai Y, Iyanagi T, Sato R (1979) Interaction between NADPH-cytochrome P-450 reductase and cytochrome P-450 in the membrane of phosphatidylcholine vesicles. *Biochim Biophys Acta* 550:341–356
  44. Black S, French JS, Williams JH Jr, Coon MJ (1979) Role of a hydrophobic polypeptide in the N-terminal region of NADPH-cytochrome P-450 reductase in complex formation with P-450LM. *Biochem Biophys Res Comm* 91:1528–1535
  45. Cojocaru V, Balali-Mood K, Sansom MS, Wade RC (2012) Structure and dynamics of the membrane-bound cytochrome P450 2C9. *PLoS Comput Biol* 7: e1002152
  46. Gilep A, Guryev OL, Usanov SA, Estabrook RW (2001) An enzymatically active chimeric protein containing the hydrophilic form of NADPH-cytochrome P450 reductase fused to the membrane-binding

- domain of cytochrome  $b_5$ . *Biochem Biophys Res Comm* 284:937–941
47. Venkateswarlu K, Lamb DC, Kelly DE, Manning NJ, Kelly SL (1998) The N-terminal membrane domain of yeast NADPH-cytochrome P450 CYP, oxidoreductase is not required for catalytic activity in sterol biosynthesis or in reconstitution of CYP activity. *J Biol Chem* 273:4492–4496
  48. Blanck J, Smettan G, Ristau O, Ingelman-Sundberg M, Ruckpaul K (1984) Mechanism of rate control of the NADPH-dependent reduction of cytochrome P-450 by lipids in reconstituted phospholipid vesicles. *Eur J Biochem* 144:509–513
  49. Vermilion JL, Ballou DP, Massey V, Coon MJ (1981) Separate roles for FMN and FAD in catalysis by liver microsomal NADPH-cytochrome P-450 reductase. *J Biol Chem* 256:266–277
  50. Shen AL, Porter TD, Wilson TE, Kasper CB (1989) Structural analysis of the FMN binding domain of NADPH-cytochrome P-450 oxidoreductase by site-directed mutagenesis. *J Biol Chem* 264:7584–7589
  51. Marohnic CC, Panda SP, McCammon K, Rueff J, Masters BS, Kranendonk M (2010) Human cytochrome P450 oxidoreductase deficiency caused by the Y181D mutation: molecular consequences and rescue of defect. *Drug Metab Disp* 38:332–340
  52. Nicolo C, Fluck CE, Mullis PE, Pandey AV (2010) Restoration of mutant cytochrome P450 reductase activity by external flavin. *Mol Cell Endo* 321:245–252
  53. Hamdane D, Xia C, Im SC, Zhang H, Kim JJ, Waskell L (2009) Structure and function of an NADPH-cytochrome P450 oxidoreductase in an open conformation capable of reducing cytochrome P450. *J Biol Chem* 284:11374–11384
  54. Bridges A, Gruenke L, Chang YT, Vakser IA, Loew G, Waskell L (1998) Identification of the binding site on cytochrome P450 2B4 for cytochrome  $b_5$  and cytochrome P450 reductase. *J Biol Chem* 273:17036–17049
  55. Im SC, Waskell L (2011) The interaction of microsomal cytochrome P450 2B4 with its redox partners, cytochrome P450 reductase and cytochrome  $b_5$ . *Arch Biochem Biophys* 507:144–153
  56. Johnson EF, Wester MR, Stout CD (2002) The structure of microsomal cytochrome P450 2C5: a steroid and drug metabolizing enzyme. *Endo Res* 28:435–441
  57. Nisimoto Y (1986) Localization of cytochrome c-binding domain on NADPH-cytochrome P-450 reductase. *J Biol Chem* 261:14232–14239
  58. Nisimoto Y, Otsuka-Murakami H (1988) Cytochrome  $b_5$ , cytochrome c, and cytochrome P-450 interactions with NADPH cytochrome P-450 reductase in phospholipid vesicles. *Biochemistry* 27:5869–5876
  59. Shen AL, Kasper CB (1995) Role of acidic residues in the interaction of NADPH-cytochrome P450 oxidoreductase with cytochrome P450 and cytochrome c. *J Biol Chem* 270:27475–27480
  60. Strobel HW, Hodgson AV, Shen SJ (1995) NADPH cytochrome P450 reductase and its structural and functional domains. In: Ortiz de Montellano PR (ed) *Cytochrome P450: structure, mechanism, and biochemistry*, 2nd edn. Plenum, New York
  61. Jang HH, Jamakhandi AP, Sullivan SZ, Yun CH, Hollenberg PF, Miller GP (2010) Beta sheet 2-alpha helix C loop of cytochrome P450 reductase serves as a docking site for redox partners. *Biochim Biophys Acta* 1804:1285–1293
  62. Hlavica P, Schulze J, Lewis DFV (2003) Functional interaction of cytochrome P450 with its redox partners: a critical assessment and update of the topology of predicted contact regions. *J Inorg Biochem* 96:279–297
  63. Huang WC, Ellis J, Moody PC, Raven EL, Roberts GC (2013) Redox-linked domain movements in the catalytic cycle of cytochrome P450 reductase. *Structure* 21:1581–1589
  64. Kanaan C, Zhang H, Shea EV, Hollenberg PF (2011) Uncovering the role of hydrophobic residues in cytochrome P450-cytochrome P450 reductase interactions. *Biochemistry* 50:3957–3967
  65. Miwa GT, West SB, Huang MT, Lu AY (1979) Studies on the association of cytochrome P-450 and NADPH cytochrome c reductase during catalysis in a reconstituted hydroxylating system. *J Biol Chem* 254:5695–5700
  66. Jamakhandi AP, Kuzmic P, Sanders DE, Miller GP (2007) Global analysis of protein-protein interactions reveals multiple CYP2E1-reductase complexes. *Biochemistry* 46:10192–10201
  67. Reed JR, Cawley GF, Backes WL (2011) Inhibition of cytochrome P450 1A2-mediated metabolism and production of reactive oxygen species by heme oxygenase-1 in rat liver microsomes. *Drug Metab Lett* 5:6–16
  68. Kurzban GP, Strobel HW (1986) Purification of flavin mononucleotide-dependent and flavin-adenine dinucleotide-dependent reduced nicotinamide-adenine dinucleotide phosphate-cytochrome P-450 reductase by high-performance liquid chromatography on hydroxyapatite. *J Chromatogr* 358:296–301
  69. Narayanasami R, Nishimura JS, McMillan K, Roman LJ, Shea TM, Robida AM, Horowitz PM, Masters BS (1997) The influence of chaotropic reagents on neuronal nitric oxide synthase and its flavoprotein module. Urea and guanidine hydrochloride stimulate NADPH-cytochrome c reductase activity of both proteins. *Nitric oxide Biol Chem* 1:39–49
  70. Narayanasami R, Horowitz PM, Masters BS (1995) Flavin-binding and protein structural integrity studies on NADPH-cytochrome P450 reductase are consistent with the presence of distinct domain. *Arch Biochem Biophys* 316:267–274
  71. Shen AL, Kasper CB (2000) Differential contributions of NADPH-cytochrome P450 oxidoreductase FAD binding site residues to flavin binding and catalysis. *J Biol Chem* 275:41087–41091
  72. Shen AL, Kasper CB (1996) Role of Ser457 of NADPH-cytochrome P450 oxidoreductase in catalysis and control of FAD oxidation-reduction potential. *Biochemistry* 35:9451–9459

73. Shen AL, Sem DS, Kasper CB (1999) Mechanistic studies on the reductive half-reaction of NADPH-cytochrome P450 oxidoreductase. *J Biol Chem* 274:5391–5398
74. Hubbard PA, Shen AL, Paschke R, Kasper CB, Kim JJ (2001) NADPH-cytochrome P450 oxidoreductase: structural basis for hydride and electron transfer. *J Biol Chem* 276:29163–29170
75. Deng Z, Aliverti A, Zanetti G, Arakaki AK, Ottado J, Orellano EG, Calcaterra NB, Ceccarelli EA, Carrillo N, Karplus PA (1999) A productive NADP<sup>+</sup> binding mode of ferredoxin-NADP<sup>+</sup> reductase revealed by protein engineering and crystallographic studies. *Nat Struct Biol* 6:847–853
76. Tejero J, Perez-Dorado I, Maya C, Martinez-Julvez M, Sanz-Aparicio J, Gomez-Moreno C, Hermoso JA, Medina M (2005) C-terminal tyrosine of ferredoxin-NADP<sup>+</sup> reductase in hydride transfer processes with NAD(P)<sup>+</sup>/H. *Biochemistry* 44:13477–13490
77. Sem DS, Kasper CB (1993) Interaction with arginine 597 of NADPH-cytochrome P-450 oxidoreductase is a primary source of the uniform binding energy used to discriminate between NADPH and NADH. *Biochemistry* 32:11548–11558
78. Gutierrez A, Doehr O, Paine M, Wolf CR, Scrutton NS, Roberts GC (2000) Trp676 facilitates nicotinamide coenzyme exchange in the reductive half-reaction of human cytochrome P450 reductase: properties of the soluble W676H and W676A mutant reductases. *Biochemistry* 39:15990–15999
79. Elmore CL, Porter TD (2002) Modification of the nucleotide cofactor-binding site of cytochrome P-450 reductase to enhance turnover with NADH *in vivo*. *J Biol Chem* 277:48960–48964
80. Xia C, Hamdane D, Shen AL, Choi V, Kasper CB, Pearl NM, Zhang H, Im SC, Waskell L, Kim JJ (2011) Conformational changes of NADPH-cytochrome P450 oxidoreductase are essential for catalysis and cofactor binding. *J Biol Chem* 286:16246–16260
81. Xia C, Panda SP, Marohnic CC, Martasek P, Masters BS, Kim JJ (2011) Structural basis for human NADPH-cytochrome P450 oxidoreductase deficiency. *Proc Natl Acad Sci U S A* 108:13486–13491
82. Page CC, Moser CC, Chen X, Dutton PL (1999) Natural engineering principles of electron tunneling in biological oxidation-reduction. *Nature* 402:47–52
83. Bhattacharyya AK, Lipka JJ, Waskell L, Tollin G (1991) Laser flash photolysis studies of the reduction kinetics of NADPH:cytochrome P-450 reductase. *Biochemistry* 30:759–765
84. Gutierrez A, Paine M, Wolf CR, Scrutton NS, Roberts GC (2002) Relaxation kinetics of cytochrome P450 reductase: internal electron transfer is limited by conformational change and regulated by coenzyme binding. *Biochemistry* 41:4626–4637
85. Zhao Q, Modi S, Smith G, Paine M, McDonagh PD, Wolf CR, Tew D, Lian LY, Roberts GC, Driessen HP (1999) Crystal structure of the FMN-binding domain of human cytochrome P450 reductase at 1.93 Å resolution. *Protein Sci* 8:298–306
86. Kim JJ, Shen AL, Xia C (2012) Structure and catalytic mechanism of NADPH-cytochrome P450 oxidoreductase: a prototype of the diflavin oxidoreductase family of enzymes. In: Hille R, Miller S, Palfey B (eds) *Handbook of flavoproteins*, vol 2. de Gruyter, Berlin, pp 73–101
87. Schilder J, Ubbink M (2013) Formation of transient protein complexes. *Curr Opin Struct Biol* 23:911–918
88. Sem DS, Kasper CB (1995) Effect of ionic strength on the kinetic mechanism and relative rate limitation of steps in the model NADPH-cytochrome P450 oxidoreductase reaction with cytochrome *c*. *Biochemistry* 34:12768–12774
89. Sevrioukova IF, Li H, Zhang H, Peterson JA, Poulos TL (1999) Structure of a cytochrome P450-redox partner electron-transfer complex. *Proc Natl Acad Sci U S A* 96:1863–1868
90. Sugishima M, Sato H, Higashimoto Y, Harada J, Wada K, Fukuyama K, Noguchi M (2014) Structural basis for the electron transfer from an open form of NADPH-cytochrome P450 oxidoreductase to heme oxygenase. *Proc Natl Acad Sci U S A* 111:2524–2529
91. Lamb DC, Kim Y, Yermalitskaya LV, Yermalitsky VN, Lepesheva GI, Kelly SL, Waterman MR, Podust LM (2006) A second FMN binding site in yeast NADPH-cytochrome P450 reductase suggests a mechanism of electron transfer by diflavin reductases. *Structure* 14:51–61
92. Gruez A, Pignol D, Zeghouf M, Coves J, Fontecave M, Ferrer JL, Fontecilla-Camps JC (2000) Four crystal structures of the 60 kDa flavoprotein monomer of the sulfite reductase indicate a disordered flavodoxin-like module. *J Mol Biol* 299:199–212
93. Aigrain L, Pompon D, Morera S, Truan G (2009) Structure of the open conformation of a functional chimeric NADPH cytochrome P450 reductase. *EMBO Rep* 10:742–747
94. Hay S, Brenner S, Khara B, Quinn AM, Rigby SE, Scrutton NS (2010) Nature of the energy landscape for gated electron transfer in a dynamic redox protein. *J Am Chem Soc* 132:9738–9745
95. Ellis J, Gutierrez A, Barsukov IL, Huang WC, Grossmann JG, Roberts GC (2009) Domain motion in cytochrome P450 reductase: conformational equilibria revealed by NMR and small-angle x-ray scattering. *J Biol Chem* 284:36628–36637
96. Vincent B, Morellet N, Fatemi F, Aigrain L, Truan G, Guittet E, Lescop E (2012) The closed and compact domain organization of the 70-kDa human cytochrome P450 reductase in its oxidized state as revealed by NMR. *J Mol Biol* 420:296–309
97. Pudney CR, Khara B, Johannissen LO, Scrutton NS (2011) Coupled motions direct electrons along human microsomal P450 chains. *PLoS Biol* 9:e1001222
98. Niedenthal R, Riles L, Guldener U, Klein S, Johnston M, Hegemann J (1999) Systematic analysis of *S. cerevisiae* chromosome VIII genes. *Yeast* 15:1775–1796
99. Benenati G, Penkov S, Müller-Reichert T, Entchev EV, Kurzchalia TV (2009) Two cytochrome P450s in *Caenorhabditis elegans* are essential for the organiza-

- tion of eggshell, correct execution of meiosis and the polarization of embryo. *Mech Dev* 126:382–393
100. Rappleye CA, Tagawa A, Le Bot N, Ahringer J, Aronian RV (2003) Involvement of fatty acid pathways and cortical interaction of the pronuclear complex in *Caenorhabditis elegans* embryonic polarity. *BMC Dev Biol* 3:8
  101. Shen AL, O'Leary KA, Kasper CB (2002) Association of multiple developmental defects and embryonic lethality with loss of microsomal NADPH-cytochrome P450 oxidoreductase. *J Biol Chem* 277:6536–6541
  102. Otto DM, Henderson CJ, Carrie D, Davey M, Gundersen TE, Blomhoff R, Adams RH, Tickle C, Wolf CR (2003) Identification of novel roles of the cytochrome P450 system in early embryogenesis: effects on vasculogenesis and retinoic acid homeostasis. *Mol Cell Biol* 23:6103–6116
  103. Gu J, Cui H, Behr M, Zhang L, Zhang QY, Yang W, Hinson JA, Ding X (2005) *In vivo* mechanisms of tissue-selective drug toxicity: effects of liver-specific knockout of the NADPH-cytochrome P450 reductase gene on acetaminophen toxicity in kidney, lung, and nasal mucosa. *Mol Pharm* 67:623–630
  104. Gu J, Weng Y, Zhang QY, Cui H, Behr M, Wu L, Yang W, Zhang L, Ding X (2003) Liver-specific deletion of the NADPH-cytochrome P450 reductase gene: impact on plasma cholesterol homeostasis and the function and regulation of microsomal cytochrome P450 and heme oxygenase. *J Biol Chem* 278:25895–25901
  105. Henderson CJ, Otto DM, Carrie D, Magnuson MA, McLaren AW, Rosewell I, Wolf CR (2003) Inactivation of the hepatic cytochrome P450 system by conditional deletion of hepatic cytochrome P450 reductase. *J Biol Chem* 278:13480–13486
  106. Stiborová M, Arlt VM, Henderson CJ, Wolf CR, Kotrbová V, Moserová M, Hudeček J, Phillips DH, Frei E (2008) Role of hepatic cytochromes P450 in bioactivation of the anticancer drug ellipticine: studies with the hepatic NADPH:cytochrome P450 reductase null mouse. *Toxic Appl Pharm* 226:318–327
  107. Riddick DS, Ding X, Wolf CR, Porter TD, Pandey AV, Zhang QY, Gu J, Finn RD, Ronseaux S, McLaughlin LA, Henderson CJ, Zou L, Fluck CE (2013) NADPH-cytochrome P450 oxidoreductase: roles in physiology, pharmacology, and toxicology. *Drug Metab Disp* 41:12–23
  108. Flück CE, Pandey AV, Arlt W, Okuhara K, Verge CF, Jabs EW, Mendonça BB, Fujieda K, Miller WL (2004) Mutant P450 oxidoreductase causes disordered steroidogenesis with and without Antley-Bixler syndrome. *Nat Genet* 36:228–230
  109. Tee MK, Damm I, Miller WL (2011) Transcriptional regulation of the human P450 oxidoreductase gene: hormonal regulation and influence of promoter polymorphisms. *Mol Endocrinol* 25:715–731
  110. Soneda S, Yazawa T, Fukami M, Adachi M, Mizota M, Fujieda K, Miyamoto K, Ogata T (2011) Proximal promoter of the cytochrome P450 oxidoreductase gene: identification of microdeletions involving the untranslated exon I and critical function of the SP1 binding sites. *J Clin Endocrinol Metab* 96:E1881–1887
  111. Miller WL, Huang N, Pandey AV, Fluck CE, Agrawal V (2005) P450 oxidoreductase deficiency: a new disorder of steroidogenesis. *Ann N Y Acad Sci* 1061:100–108
  112. Fluck CE, Pandey AV (2011) Clinical and biochemical consequences of P450 oxidoreductase deficiency. *Endo Dev* 20:63–79
  113. Pandey AV, Fluck CE (2013) NADPH P450 oxidoreductase: structure, function, and pathology of diseases. *Pharmacol Ther* 138:229–254
  114. Fukami M, Horikawa R, Nagai T, Tanaka T, Naiki Y, Sato N, Okuyama T, Nakai H, Soneda S, Tachibana K, Matsuo N, Sato S, Homma K, Nishimura G, Hasegawa T, Ogata T (2005) Cytochrome P450 oxidoreductase gene mutations and Antley-Bixler syndrome with abnormal genitalia and/or impaired steroidogenesis: molecular and clinical studies in 10 patients. *J Clin Endocrinol Metab* 90:414–426
  115. Yanagibashi K, Hall PF (1986) Role of electron transport in the regulation of the lyase activity of C21 side-chain cleavage P-450 from porcine adrenal and testicular microsomes. *J Biol Chem* 261:8429–8433
  116. Lin D, Black SM, Nagahama Y, Miller WL (1993) Steroid 17 alpha-hydroxylase and 17,20-lyase activities of P450c17: contributions of serine106 and P450 reductase. *Endocrinology* 132:2498–2506
  117. Panda SP, Guntur AR, Polusani SR, Fajardo RJ, Gakunga PT, Roman LJ, Masters BS (2013) Conditional deletion of cytochrome P450 reductase in osteoprogenitor cells affects long bone and skull development in mice recapitulating Antley-Bixler syndrome: role of a redox enzyme in development. *PLoS ONE* 8:e75638
  118. Huang N, Pandey AV, Agrawal V, Reardon W, Lapunzina PD, Mowat D, Jabs EW, Van Vliet G, Sack J, Fluck CE, Miller WL (2005) Diversity and function of mutations in P450 oxidoreductase in patients with Antley-Bixler syndrome and disordered steroidogenesis. *Am J Hum Genet* 76:729–749
  119. Marohnic CC, Martásek PS, Masters BS (2006) Diminished FAD binding in the Y459H and V492E Antley-Bixler syndrome mutants of human cytochrome P450 reductase. *J Biol Chem* 281:35975–35982
  120. Hart SN, Nakamoto K, Wesselman C, Li Y, Zhong XB (2008) Genetic polymorphisms in cytochrome P450 oxidoreductase influence microsomal P450-catalyzed drug metabolism. *Pharmacogenet Genomics* 18:11–24
  121. Gomes AM, Klein K, Turpeinen M, Schaeffeler E, Schwab M, Zanger UM (2009) Pharmacogenomics of human liver cytochrome P450 oxidoreductase: multifactorial analysis and impact on microsomal drug oxidation. *Pharmacogenomics* 10:579–599
  122. Huang N, Agrawal V, Giacomini KM, Miller WL (2008) Genetics of P450 oxidoreductase: sequence variation in 842 individuals of four ethnicities and activities of 15 missense mutations. *Proc Natl Acad Sci U S A* 105:1733–1738



123. Agrawal V, Huang N, Miller WL (2008) Pharmacogenetics of P450 oxidoreductase: effect of sequence variants on activities of CYP1A2 and CYP2C19. *Pharmacogenet Genomics* 18:569–576
124. Agrawal V, Choi JH, Giacomini KM, Miller WL (2010) Substrate-specific modulation of CYP3A4 activity by genetic variants of cytochrome P450 oxidoreductase. *Pharmacogenet Genomics* 20:611–618
125. Sandee D, Morrissey K, Agrawal V, Tam HK, Kramer MA, Tracy TS, Giacomini KM, Miller WL (2010) Effects of genetic variants of human P450 oxidoreductase on catalysis by CYP2D6 *in vitro*. *Pharmacogenomics* 20:677–686
126. Subramanian M, Agrawal V, Sandee D, Tam HK, Miller WL, Tracy TS (2012) Effect of P450 oxidoreductase variants on the metabolism of model substrates mediated by CYP2C9.1, CYP2C9.2, and CYP2C9.3. *Pharmacogenet Genomics* 22:590–597
127. Schenkman JB, Jansson I (2003) The many roles of cytochrome b<sub>5</sub>. *Pharmacol Ther* 97:139–152
128. Ahuja S, Jahr N, Im SC, Vivekanandan S, Popovych N, LeClair SV, Huang R, Soong R, Xu J, Yamamoto K, Nanga, RP, Bridges A, Waskell L, Ramamoorthy A (2013) A model of the membrane-bound cytochrome b<sub>5</sub>-cytochrome P450 complex from NMR and mutagenesis data. *J Biol Chem* 288:22080–22095
129. Vergeres G, Waskell L (1995) Cytochrome b<sub>5</sub>: its function, structure, and membrane topology. *Biochimie* 77:604–620
130. Deng B, Parthasarathy S, Wang W-F, Gibney BR, Battaille KP, Lovell S, Benson DR, Zhu H (2010) Study of the individual cytochrome b<sub>5</sub> and cytochrome b<sub>5</sub> reductase domains of Ncb5or reveals a unique heme pocket and a possible role of the CS domain. *J Biol Chem* 285:30181–30191
131. Plitzko B, Ott G, Reichmann D, Henderson CJ, Wolf CR, Mendel R, Bittner F, Clement B, Havemeyer A (2013) The involvement of mitochondrial amidoxime reducing components 1 and 2 and mitochondrial cytochrome b<sub>5</sub> in N-reductive metabolism in human cells. *J Biol Chem* 288:20228–20237
132. Morgan ET, Coon MJ (1984) Effects of cytochrome b<sub>5</sub> on cytochrome P-450-catalyzed reactions. *Studies with manganese-substituted cytochrome b<sub>5</sub>*. *Drug Metab Dispos* 12:358–364
133. Yamazaki H, Shimada T, Martin MV, Guengerich FP (2001) Stimulation of cytochrome P450 reactions by apo-cytochrome b<sub>5</sub>: evidence against transfer of heme from cytochrome P450 3A4 to apo-cytochrome b<sub>5</sub> or heme oxygenase. *J Biol Chem* 276:30885–30891
134. Zhao C, Gao Q, Roberts AG, Shaffer SA, Doneanu CE, Xue S, Goodlett DR, Nelson SD, Atkins WM (2012) Cross-linking mass spectrometry and mutagenesis confirm the functional importance of surface interactions between CYP3A4 and holo/apo cytochrome b<sub>5</sub>. *Biochemistry* 51:9488–9500
135. McLaughlin LA, Ronseaux S, Finn RD, Henderson CJ, Wolf CR (2010) Deletion of microsomal cytochrome b<sub>5</sub> profoundly affects hepatic and extrahepatic drug metabolism. *Mol Pharmacol* 78:269–278
136. Finn RD, McLaughlin LA, Ronseaux S, Rosewell I, Houston JB, Henderson CJ, Wolf CR (2008) Defining the *in vivo* role for cytochrome b<sub>5</sub> in cytochrome P450 function through the conditional hepatic deletion of microsomal cytochrome b<sub>5</sub>. *J Biol Chem* 283:31385–31393
137. Yamazaki H, Gillam EM, Dong MS, Johnson WW, Guengerich FP, Shimada T (1997) Reconstitution of recombinant cytochrome P450 2C10(2C9), and comparison with cytochrome P450 3A4 and other forms: effects of cytochrome P450-P450 and cytochrome P450-b<sub>5</sub> interactions. *Arch Biochem Biophys* 342:329–337
138. Imai Y, Sato R (1977) The roles of cytochrome b<sub>5</sub> in a reconstituted N-demethylase system containing cytochrome P-450. *Biochem Biophys Res Commun* 75:420–426
139. Zhang H, Hamdane D, Im SC, Waskell L (2008) Cytochrome b<sub>5</sub> inhibits electron transfer from NADPH-cytochrome P450 reductase to ferric cytochrome P450 2B4. *J Biol Chem* 283:217–225
140. Henderson CJ, McLaughlin LA, Finn RD, Ronseaux S, Kapelyukh Y, Wolf CR (2014) A role for cytochrome b<sub>5</sub> in the *in vivo* disposition of anticancer and cytochrome P450 probe drugs in mice. *Drug Metab Dispos* 42:1–77
141. Hildebrandt A, Estabrook RW (1971) Evidence for the participation of cytochrome b<sub>5</sub> in hepatic microsomal mixed-function oxidation reactions. *Arch Biochem Biophys* 143:66–79
142. Page CC, Moser CC, Dutton PL (2003) Mechanism for electron transfer within and between proteins. *Curr Opin Chem Biol* 7:551–556
143. Bonsor DA, Sundberg EJ (2011) Dissecting protein-protein interactions using directed evolution. *Biochemistry* 50:2394–2402
144. Johansson MP, Blomberg MR, Sundholm D, Wikstrom M (2002) Change in electron and spin density upon electron transfer to haem. *Biochim Biophys Acta* 1553:183–187
145. Clackson T, Wells JA (1995) A hot spot of binding energy in a hormone-receptor interface. *Science* 267:383–386
146. Bogan AA, Thorn KS (1998) Anatomy of hot spots in protein interfaces. *J Mol Biol* 280:1–9
147. Crowley PB, Carrondo MA (2004) The architecture of the binding site in redox protein complexes: implications for fast dissociation. *Proteins* 55:603–612
148. Correia MA, Mannering GJ (1973) Reduced diphosphopyridine nucleotide synergism of the reduced triphosphopyridine nucleotide-dependent mixed-function oxidase system of hepatic microsomes. II. Role of the type I drug-binding site of cytochrome P-450. *Mol Pharmacol* 9:470–485
149. Zhang H, Gruenke L, Arscott D, Shen A, Kasper CB, Harris DL, Glavanovich M, Johnson R, Waskell L (2003) Determination of the rate of reduction of oxyferrous cytochrome P450 2B4 by 5-deazaFAD

- T491V cytochrome P450 reductase. *Biochemistry* 42:11594–11603
150. Guengerich FP, Ballou DP, Coon MJ (1975) Purified liver microsomal cytochrome P-450. Electron-accepting properties and oxidation-reduction potential. *J Biol Chem* 250:7405–7414
  151. Sligar SG, Cinti DL, Gibson GG, Schenkman JB (1979) Spin state control of the hepatic cytochrome P450 redox potential. *Biochem Biophys Res Commun* 90:925–932
  152. Lewis DF, Hlavica P (2000) Interactions between redox partners in various cytochrome P450 systems: functional and structural aspects. *Biochim Biophys Acta* 1460:353–374
  153. Guengerich FP (1983) Oxidation-reduction properties of rat liver cytochromes P-450 and NADPH-cytochrome P-450 reductase related to catalysis in reconstituted systems. *Biochemistry* 22:2811–2820
  154. Gorsky LD, Coon MJ (1986) Effects of conditions for reconstitution with cytochrome  $b_5$  on the formation of products in cytochrome P-450-catalyzed reactions. *Drug Metab Dispos* 14:89–96
  155. Auchus RJ, Lee TC, Miller WL (1998) Cytochrome  $b_5$  augments the 17,20-lyase activity of human P450c17 without direct electron transfer. *J Biol Chem* 273:3158–3165
  156. Yamazaki H, Johnson WW, Ueng YF, Shimada T, Guengerich FP (1996) Lack of electron transfer from cytochrome  $b_5$  in stimulation of catalytic activities of cytochrome P450 3A4. Characterization of a reconstituted cytochrome P450 3A4/NADPH-cytochrome P450 reductase system and studies with apo-cytochrome  $b_5$ . *J Biol Chem* 271:27438–27444
  157. Gruenke LD, Konopka K, Cadieu M, Waskell L (1995) The stoichiometry of the cytochrome P-450-catalyzed metabolism of methoxyflurane and benzphetamine in the presence and absence of cytochrome  $b_5$ . *J Biol Chem* 270:24707–24718
  158. Perret A, Pompon D (1998) Electron shuttle between membrane-bound cytochrome P450 3A4 and  $b_5$  rules uncoupling mechanisms. *Biochemistry* 37:11412–11424
  159. Gilep AA, Guryev OL, Usanov SA, Estabrook RW (2001) Expression, purification, and physical properties of recombinant flavocytochrome fusion proteins containing rat cytochrome  $b_5$  linked to NADPH-cytochrome P450 reductase by different membrane-binding segments. *Arch Biochem Biophys* 390:222–234
  160. Akhtar MK, Kelly SL, Kaderbhai MA (2005) Cytochrome  $b_5$  modulation of 17 $\alpha$  hydroxylase and 17–20 lyase CYP17, activities in steroidogenesis. *J Endocrinol* 187:267–274
  161. Hasemann CA, Kurumbail RG, Boddupalli SS, Peterson JA, Deisenhofer J (1995) Structure and function of cytochromes P450: a comparative analysis of three crystal structures. *Structure* 3:41–62
  162. Poulos TL, Finzel BC, Howard AJ (1987) High-resolution crystal structure of cytochrome P450cam. *J Mol Biol* 195:687–700
  163. Scott EE, White MA, He YA, Johnson EF, Stout CD, Halpert JR (2004) Structure of mammalian cytochrome P450 2B4 complexed with 4-(4-chlorophenyl)imidazole at 1.9 Å resolution: insight into the range of P450 conformations and coordination of redox partner binding. *J Biol Chem* 279:27294–27301
  164. Estrada DF, Skinner AL, Laurence JS, Scott EE (2014) Human cytochrome P450 17A1 conformational selection: modulation by ligand and cytochrome  $b_5$ . *J Biol Chem* 289:14310–14320
  165. Estrada DF, Laurence JS, Scott EE (2013) Substrate-modulated cytochrome P450 17A1 and cytochrome  $b_5$  interactions revealed by NMR. *J Biol Chem* 288:17008–17018
  166. Gao Q, Doneanu CE, Shaffer SA, Adman ET, Goodlett DR, Nelson SD (2006) Identification of the interactions between cytochrome P450 2E1 and cytochrome  $b_5$  by mass spectrometry and site-directed mutagenesis. *J Biol Chem* 281:20404–20417
  167. Koga H, Sagara Y, Yaoi T, Tsujimura M, Nakamura K, Sekimizu K, Makino R, Shimada H, Ishimura Y, Yura K, Go M, Ikeguchi I, Horiuchi T (1993) Essential role of the Arg112 residue of cytochrome P450cam for electron transfer from reduced putidaredoxin. *FEBS Lett* 331:109–113
  168. Tripathi S, Li H, Poulos TL (2013) Structural basis for effector control and redox partner recognition in cytochrome P450. *Science* 340:1227–1230
  169. Stayton PS, Sligar SG (1990) The cytochrome P-450cam binding surface as defined by site-directed mutagenesis and electrostatic modeling. *Biochemistry* 29:7381–7386
  170. Rui L, Pochapsky SS, Pochapsky T (2006) Comparison of the complexes formed by cytochrome P450<sub>CAM</sub> with cytochrome  $b_5$  and putidaredoxin, two effectors of camphor hydroxylase activity. *Biochemistry* 45:3887–3897
  171. Noble MA, Girvan HM, Smith SJ, Smith WE, Murataliev M, Guzov VM, Feyereisen R, Munro AW (2007) Analysis of the interactions of cytochrome  $b_5$  with flavocytochrome P450 BM3 and its domains. *Drug Metab Rev* 39:599–617
  172. Stayton PS, Poulos TL, Sligar SG (1989) Putidaredoxin competitively inhibits cytochrome  $b_5$ -cytochrome P-450cam association: a proposed molecular model for a cytochrome P-450cam electron-transfer complex. *Biochemistry* 28:8201–8205
  173. Jenkins CM, Waterman MR (1999) Flavodoxin as a model for the P450-interacting domain of NADPH cytochrome P450 reductase. *Drug Metab Rev* 31:195–203
  174. Geller DH, Auchus RJ, Mendonca BB, Miller WL (1997) The genetic and functional basis of isolated 17,20-lyase deficiency. *Nat Genet* 17:201–205
  175. Hong Y, Rashid R, Chen S (2011) Binding features of steroidal and nonsteroidal inhibitors. *Steroids* 76:802–806
  176. Kaspera R, Naraharisetti SB, Evangelista EA, Marcianti KD, Psaty BM, Totah RA (2011) Drug me-

- tabolism by CYP2C8.3 is determined by substrate dependent interactions with cytochrome P450 reductase and cytochrome  $b_5$ . *Biochem Pharmacol* 82:681–691
177. Nikfarjam L, Izumi S, Yamazaki T, Kominami S (2006) The interaction of cytochrome P450 17 $\alpha$  with NADPH-cytochrome P450 reductase, investigated using chemical modification and MALDI-TOF mass spectrometry. *Biochim Biophys Acta* 1764:1126–1131
178. Furuya H, Shimizu T, Hirano K, Hatano M, Fujii-Kuriyama Y, Raag R, Poulos TL (1989) Site-directed mutageneses of rat liver cytochrome P-450d: catalytic activities toward benzphetamine and 7-ethoxycoumarin. *Biochemistry* 28:6848–6857
179. Shimizu T, Tateishi T, Hatano M, Fujii-Kuriyama Y (1991) Probing the role of lysines and arginines in the catalytic function of cytochrome P450d by site-directed mutagenesis. Interaction with NADPH-cytochrome P450 reductase. *J Biol Chem* 266:3372–3375
180. Shen S, Strobel HW (1992) The role of cytochrome P450 lysine residues in the interaction between cytochrome P450IA1 and NADPH-cytochrome P450 reductase. *Arch Biochem Biophys* 294:83–90
181. Shen S, Strobel HW (1993) Role of lysine and arginine residues of cytochrome P450 in the interaction between cytochrome P4502B1 and NADPH-cytochrome P450 reductase. *Arch Biochem Biophys* 304:257–265
182. Nakamura K, Horiuchi T, Yasukochi T, Sekimizu K, Hara T, Sagara Y (1994) Significant contribution of arginine-112 and its positive charge of *Pseudomonas putida* cytochrome P-450cam in the electron transport from putidaredoxin. *Biochim Biophys Acta* 1207:40–48
183. Stayton PS, Sligar SG (1991) Structural microheterogeneity of a tryptophan residue required for efficient biological electron transfer between putidaredoxin and cytochrome P-450cam. *Biochemistry* 30:1845–1851
184. Lee MY, Borgiani P, Johansson I, Oteri F, Mkrtchian S, Falconi M, Ingelman-Sundberg M (2013) High warfarin sensitivity in carriers of CYP2C9\*35 is determined by the impaired interaction with P450 oxidoreductase. *Pharmacogenomics J* Epub prior to publication, 12/10/14. doi:10.1038/tpj.2013.41
185. Mao W, Rupasinghe SG, Zangerl AR, Berenbaum MR, Schuler MA (2007) Allelic variation in the *Depressaria pastinacella* CYP6AB3 protein enhances metabolism of plant allelochemicals by altering a proximal surface residue and potential interactions with cytochrome P450 reductase. *J Biol Chem* 282:10544–10552
186. Scott EE, He YA, Wester MR, White MA, Chin CC, Halpert JR, Johnson EF, Stout CD (2003) An open conformation of mammalian cytochrome P450 2B4 at 1.6-Å resolution. *Proc Natl Acad Sci U S A* 100:13196–13201
187. Wilderman PR, Gay SC, Jang, H-H, Zhang Q, Stout CD, Halpert JR (2012) Investigation by site-directed mutagenesis of the role of cytochrome P450 2B4 non-active-site residues in protein-ligand interactions based on crystal structures of the ligand-bound enzyme. *FEBS J* 279:1607–1620
188. Lee-Robichaud P, Akhtar ME, Wright JN, Sheikh QI, Akhtar M (2004) The cationic charges on Arg347, Arg358 and Arg449 of human cytochrome P450c17 CYP17, are essential for the enzyme's cytochrome  $b_5$ -dependent acyl-carbon cleavage activities. *J Steroid Biochem Mol Biol* 92:119–130
189. Ozols J (1989) Structure of cytochrome  $b_5$  and its topology in the microsomal membrane. *Biochim Biophys Acta* 997:121–130
190. Gostincar C, Turk M, Gunde-Cimerman N (2010) The evolution of fatty acid desaturases and cytochrome  $b_5$  in eukaryotes. *J Memb Biol* 233:63–72
191. Peng HM, Auchus RJ (2013) The action of cytochrome  $b_5$  on CYP2E1 and CYP2C19 activities requires anionic residues D58 and D65. *Biochemistry* 52:210–220
192. Peng HM, Auchus RJ (2014) Two surfaces of cytochrome  $b_5$  with major and minor contributions to CYP3A4-catalyzed steroid and nifedipine oxygenation chemistries. *Arch Biochem Biophys* 541:53–60
193. Naffin-Olivos JL, Auchus RJ (2006) Human cytochrome  $b_5$  requires residues E48 and E49 to stimulate the 17,20-lyase activity of cytochrome P450c17. *Biochemistry* 45:755–762
194. Chudaev MV, Gilep AA, Usanov SA (2001) Site-directed mutagenesis of cytochrome  $b_5$  for studies of its interaction with cytochrome P450. *Biochemistry (Moscow)* 66:667–681
195. Peterson JA, Ebel RE, O'Keeffe DH, Matsubara T, Estabrook RW (1976) Temperature dependence of cytochrome P-450 reduction. A model for NADPH-cytochrome P-450 reductase:cytochrome P-450 interaction. *J Biol Chem* 251:4010–4016
196. Zhang H, Im S-C, Waskell L (2007) Cytochrome  $b_5$  increases the rate of product formation by cytochrome P450 2B4 and competes with cytochrome P450 reductase for a binding site on cytochrome P450 2B4. *J Biol Chem* 282:29766–29776
197. Murataliev MB, Guzov VM, Walker FA, Feyereisen R (2008) P450 reductase and cytochrome  $b_5$  interactions with cytochrome P450: effects on house fly CYP6A1 catalysis. *Insect Biochem Mol Biol* 38:1008–1015
198. Pompon D, Coon MJ (1984) On the mechanism of action of cytochrome P-450. Oxidation and reduction of the ferrous dioxygen complex of liver microsomal cytochrome P-450 by cytochrome  $b_5$ . *J Biol Chem* 259:15377–15385
199. Bonfils C, Balny C, Maurel P (1981) Direct evidence for electron transfer from ferrous cytochrome  $b_5$  to the oxyferrous intermediate of liver microsomal cytochrome P-450 LM2. *J Biol Chem* 256:9457–9465
200. Tamburini PP, Schenkman JB (1987) Purification to homogeneity and enzymological characterization of a functional covalent complex composed of cy-

- tochromes P-450 isozyme 2 and  $b_5$  from rabbit liver. *Proc Natl Acad Sci U S A* 84:11–15
201. Yamazaki H, Nakamura M, Komatsu T, Ohyama K, Hatanaka N, Asahi S, Shimada N, Guengerich FP, Shimada T, Nakajima M, Yokoi T (2002) Roles of NADPH-P450 reductase and apo- and holo-cytochrome  $b_5$  on xenobiotic oxidations catalyzed by 12 recombinant human cytochrome P450s expressed in membranes of *Escherichia coli*. *Protein Expr Purif* 24:329–337
202. Moore CD, Al-Misky ON, Lecomte JTJ (1991) Similarities in structure between holocytochrome  $b_5$  and apocytochrome  $b_5$ : NMR studies of the histidine residues. *Biochemistry* 30:8357–8365
203. Canova-Davis E, Waskell L (1984) The identification of the heat-stable microsomal protein required for methoxyflurane metabolism as cytochrome  $b_5$ . *J Biol Chem* 259:2541–2546
204. Gilep AA, Guryev OL, Usanov SA, Estabrook RW (2001) Apo-cytochrome  $b_5$  as an indicator of changes in heme accessibility: preliminary studies with cytochrome P450 3A4. *J Inorg Biochem* 87:237–244
205. Guryev OL, Gilep AA, Usanov SA, Estabrook RW (2001) Interaction of apo-cytochrome  $b_5$  with cytochromes P4503A4 and A: relevance of heme transfer reactions. *Biochemistry* 40:5018–5031
206. Canova-Davis E, Chiang JY, Waskell L (1985) Obligatory role of cytochrome  $b_5$  in the microsomal metabolism of methoxyflurane. *Biochem Pharmacol* 34:1907–1912
207. Reed JR, Hollenberg PF (2003) Examining the mechanism of stimulation of cytochrome P450 by cytochrome  $b_5$ : the effect of cytochrome  $b_5$  on the interaction between cytochrome P450 2B4 and P450 reductase. *J Inorg Biochem* 97:265–275
208. Idkowiak J, Randell T, Dhir V, Patel P, Shackleton CH, Taylor NF, Krone N, Arlt W (2012) A missense mutation in the human cytochrome  $b_5$  gene causes 46,XY disorder of sex development due to true isolated 17,20 lyase deficiency. *J Clin Endo Metab* 97:E465–475



<http://www.springer.com/978-3-319-12107-9>

Cytochrome P450

Structure, Mechanism, and Biochemistry

Ortiz de Montellano, P.R. (Ed.)

2015, X, 912 p. 243 illus., 80 illus. in color., Hardcover

ISBN: 978-3-319-12107-9